Computational Materials Discovery

Artem R. Oganov

Beginning of a revolution in materials science

First examples of predicted and confirmed energy materials (Jain et al., 2016)

Table 1 | **Density functional theory predictions of energy-related materials that were confirmed by experiments**

Year	Material	Description	Refs
Li-ion batteries			
1998	$Li(Co_xAl_{1-x})O_2$	Al mixing to raise voltage	18
2006	$Li(Mn_{0.5}Ni_{0.5})O_2$	Li–Na ion exchange from the Na complex used to form the Li complex to improve Li–Ni ordering and achieve larger layer spacing	24
2011	$LiMnBO_3$	First use of the monoclinic phase as a cathode material	27
2011	$LiMPO_4CO_3$ (M = transition metal)	New class of sidorenkite-based cathode materials synthesized by Na ion-exchange	30,33,34
2012	$Li_3V_2(P_2O_7)_3(PO_4)_2$	New compound for cathodes	28
2012–2013	$Li_{10}SnP_2S_{12}$	New superionic conductor composition for solid-state electrolytes	25,143
2015	$Mo_2TiC_2T_x$ (2D)	2D material identified as an anode material; can also be used as a capacitor	37
Hydrogen production and storage			
1998	NiAu alloy	Catalyst for steam reforming to produce H_2 while preventing graphite build-up	39
2006	BiPt alloy	Cheaper and potentially better-performing H_2 production catalyst than pure Pt	40
2006–2010	$LiNH_2$:MgH_2 (1:1)	H_2 storage mixture; performance found to depend on ball milling procedure	47–49
2014	NiGa alloy	Catalyst that uses H_2 to reduce CO_2 into methanol as a liquid fuel, with lower production of CO than conventional Cu, ZnO and Al_2O_3 catalysts	144
2015	$Mn_2V_2O_7$	Solar water-splitting material; experiments showed photocurrent under specific electrochemical conditions but indicated that achieving efficient oxygen evolution will require a catalyst	42
Thermoelectrics			
2006	LiZnSb	n-Type compound suggested but only p-type could be synthesized	97
2006–2007	$FeSb_2$	Very high Seebeck coefficient and power factor achieved but low *ZT* because of high lattice thermal conductivity	106,107
2015	$TmAgTe_2$	Very low thermal conductivity achieved and moderate *ZT* (0.35) demonstrated, but impractical choice of elements	101
Photovoltaics			
2007	PCDTBT	Candidate copolymer donor material with high power conversion efficiency for bulk-heterojunction organic photovoltaic solar cells	89
2014	Organic dyes	New class of organic dyes for dye-sensitized solar cells	145
2013–2015	Ba_2BiTaO_6	p-Type transparent conducting oxide that utilizes alignment between Bi 6*s* and O 2*p* states	91,92
2014	TaIrGe	Unconventional p-type half-Heusler transparent conducting oxide composed of all heavy metal atoms	93
Superconductors			
1984–1985	Si (high-pressure)	Superconductivity hypothesized based on high density of states (DOS) near the Fermi level; superconductivity verified at 15 GPa and <8.2 K	56,57
1991–2003	Li (high-pressure)	Superconductivity verified at pressures above 20 GPa and temperatures <20 K	58–63
2010–2013	FeB_4 (high-pressure)	Orthorhombic *Pnmn* structure, synthesized at 8 GPa, shows behaviour indicative of superconductivity below 3 K and 1 atm	64,65
2014–2015	H_2S (high-pressure)	Predicted *P*1 or *Cmca* structure but unconfirmed by experiments; synthesized at 90 GPa, shows behaviour indicative of superconductivity at 203 K	66,67
Capacitors			
2014	Polymers for dielectric applications	267 polymers screened for dielectric constants and bandgaps; polyurea, polyimide and polythiourea synthesized with polyurea, in particular, showing very low dielectric loss	102
2015	Variants of polythiourea	Variation of the chemical design of polythiourea and experimental validation reaching a dielectric constant of 4.5 and energy densities of 10 J cm^{-3}	105

Structure is the basis for understanding materials and their properties

The Nobel Prize in Physics 1914

"for his discovery of the diffraction of X-rays by crystals"

Max von Laue

The Nobel Prize in Physics 1915

"for their services in the analysis of crystal structure by means of X-rays"

Sir William Henry Bragg

William Lawrence Bragg

The Nobel Prize in Chemistry 1985

"for their outstanding achievements in the development of direct methods for the determination of crystal structures"

Herbert A. Hauptman

Jerome Karle

(from http://nobelprize.org)

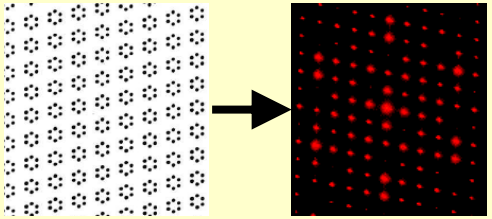

Structure Diffraction

Zincblende ZnS.

One of the first structures solved by Braggs in 1913.

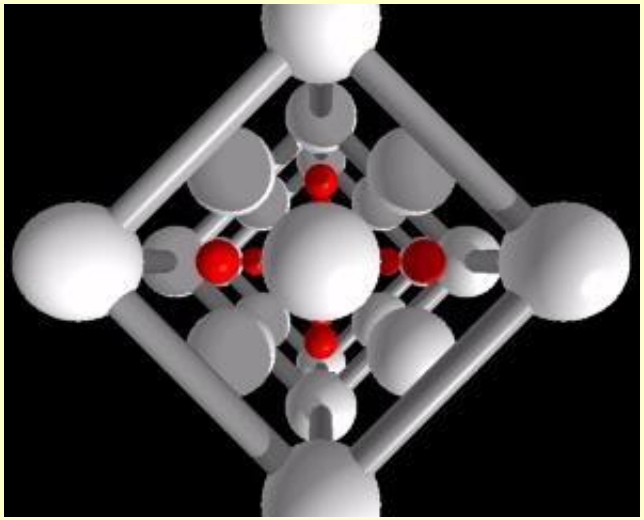

Acc. Chem. Res. **1994,** *27,* 309−314

Are Crystal Structures Predictable?

ANGELO GAVEZZOTTI*

"No": by just writing down this concise statement, in what would be the first one-word paper in the chemical literature, one could safely summarize the present state of affairs

Need to find GLOBAL energy minimum.

Trying all structures is impossible:

$$C = \frac{1}{(V/\delta^3)} \frac{(V/\delta^3)!}{[(V/\delta^3) - N]!N!}$$

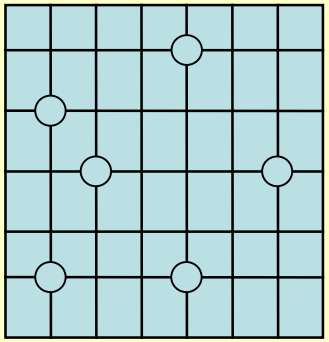

N_{atoms}	Variants	CPU time
1	**1**	**1 sec.**
10	**10^{11}**	**10^{3} yrs.**
20	**10^{25}**	**10^{17} yrs.**
30	**10^{39}**	**10^{31} yrs.**

RESEARCH NEWS

Crystal structure prediction – evolutionary or revolutionary crystallography?

S. L. Chaplot and K. R. Rao CURRENT SCIENCE, VOL. 91, NO. 11, 10 DECEMBER 2006

Overview of USPEX (Oganov & Glass, *J.Chem.Phys.* 2006)

The USPEX project
(Universal Structure Prediction: Evolutionary Xtallography)

http://uspex-team.org

[Oganov A.R., Glass C.W., *J.Chem.Phys.* 124, 244704 (2006)]

- Combination of evolutionary algorithm and quantum-mechanical calculations.
- >3700 users.

- Solves «intractable» problem of structure prediction
-3D, 2D, 1D, 0D –systems,
-prediction of phase transition mechanisms.

Quantun-mechanical calculations (density functional theory):

$$(-\frac{\nabla^2}{2}+v_{e-n}[\rho(\mathbf{r})]+v_H[\rho(\mathbf{r})]+v_{xc}[\rho(\mathbf{r})])\phi_i(\mathbf{r})=\varepsilon_i\phi_i(\mathbf{r})$$

$$E_{GGA,\mathrm{xc}}=\int \mathrm{d}\mathbf{r}\, F_{\mathrm{xc}}(\rho,\frac{|\nabla\rho|}{2k_{\mathrm{F}}\rho(\mathbf{r})})\rho(\mathbf{r})e_{\mathrm{x}}[\rho(\mathbf{r})]$$

E.Schroedinger

W. Kohn

Computer helps us to discover new science

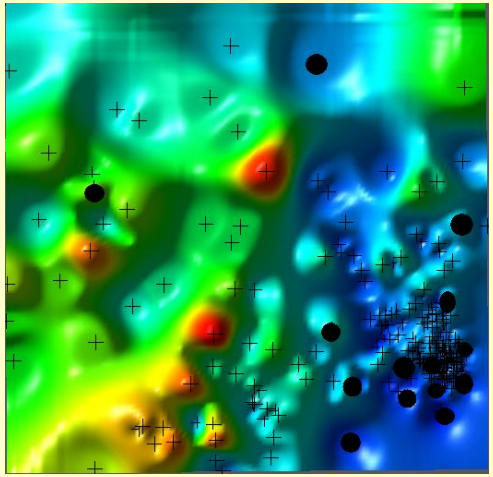

I. Predicting crystal structures by evolution

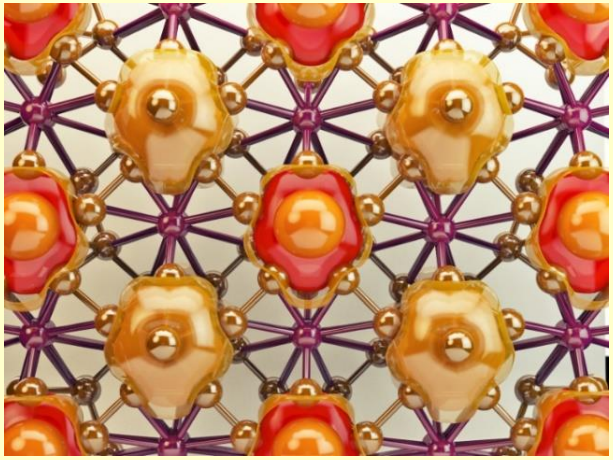

II. New materials and phenomena

Most results – USPEX+VASP (PAW-PBE).

I. Predicting structures by evolution

(Oganov & Glass, *J. Chem. Phys.* 2006)

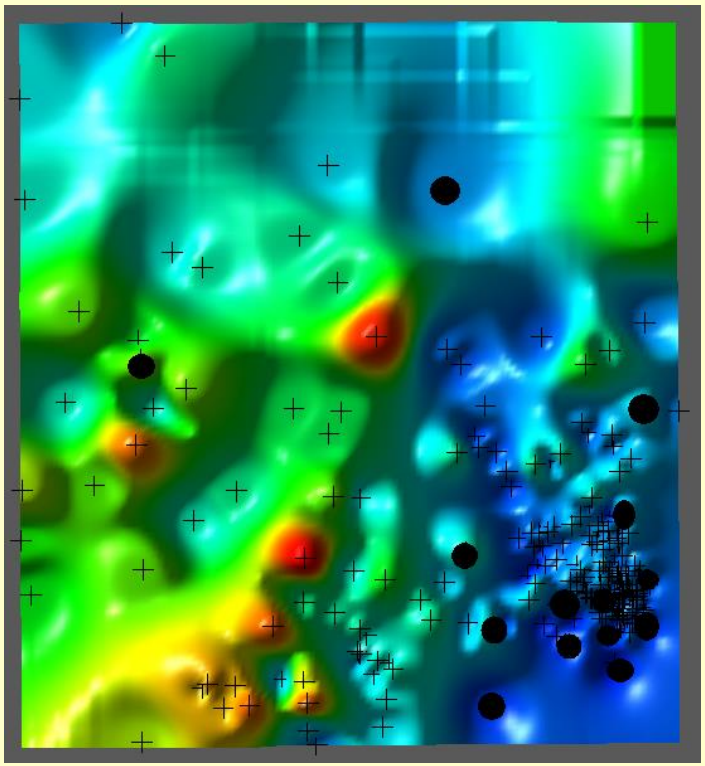

Evolution "zooms in" on the most promising areas of search space

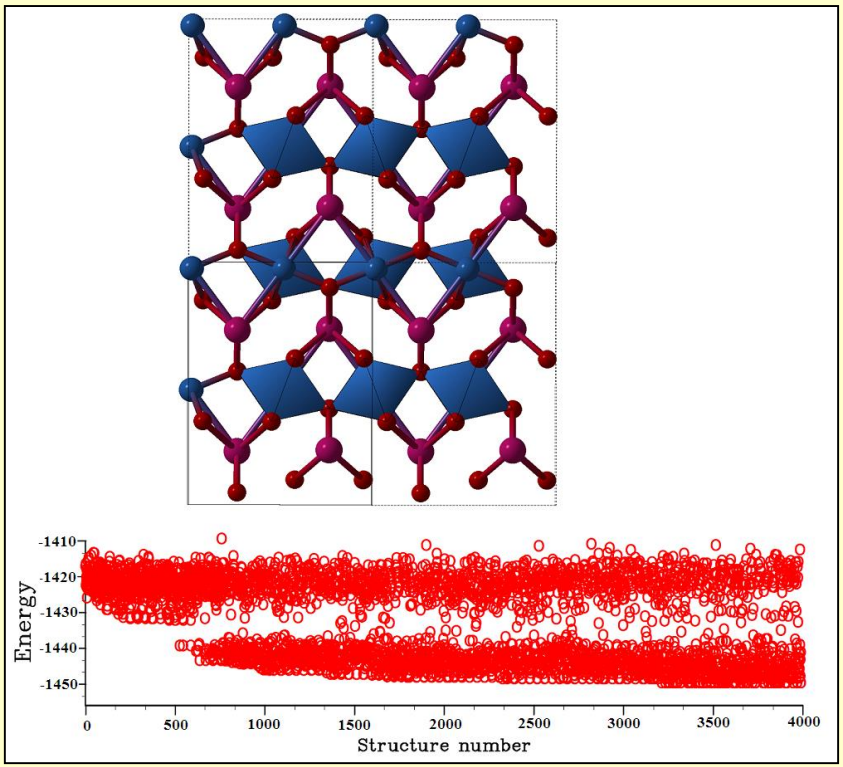

Simulation discovers increasingly better solutions

USPEX
(Universal Structure Predictor: Evolutionary Xtallography)

- (Random) initial population
- Evaluate structures by relaxed (free) energy
- Select lowest-energy structures as parents for new generation
- Standard variation operators:

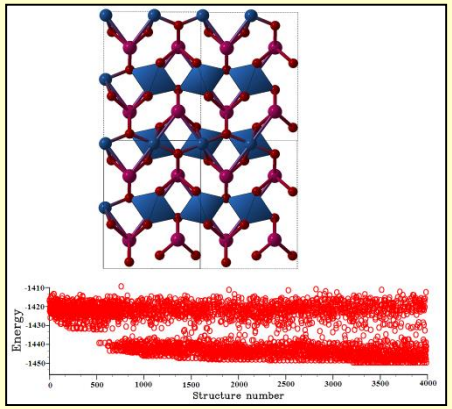

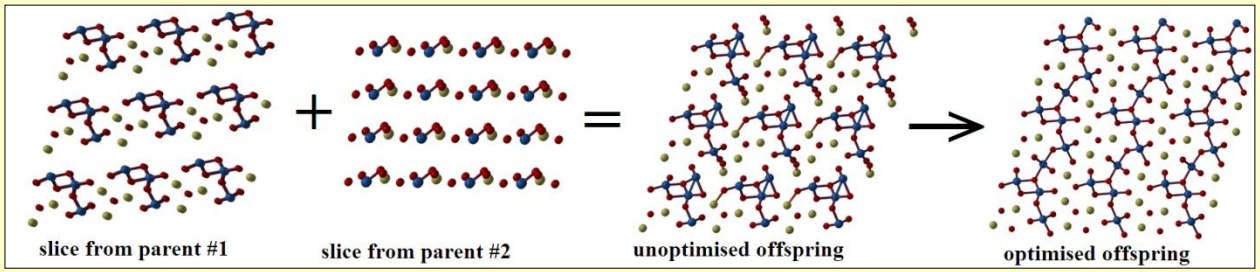

(1) Heredity (crossover)

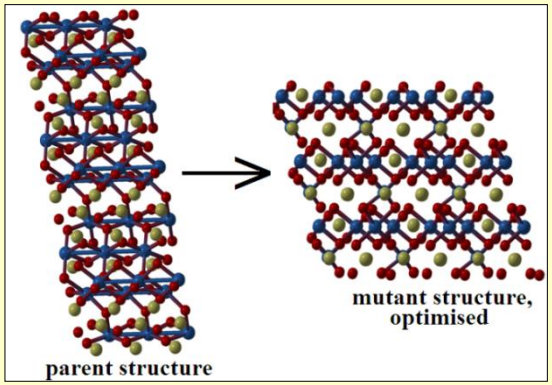

(2) Lattice mutation

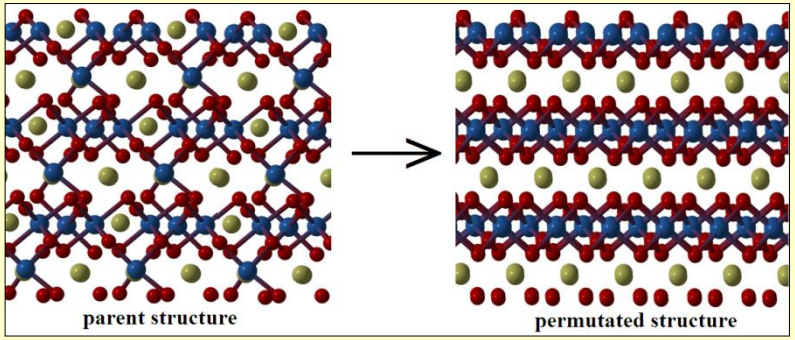

(3) Permutation

+(4) Transmutation, +(5) Rotational mutation, +(6) Soft-mode mutation, +...

Enhance algorithm with *local* knowledge

$$F_{AB}(R) = \sum_{A_i,\text{cell}} \sum_{B_j} \frac{\delta(R - R_{ij})}{4\pi R_{ij}^2 \frac{N_A N_B}{V} \Delta} - 1 = g_{AB}(R) - 1$$

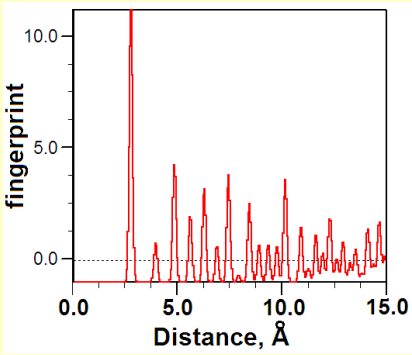

Fingerprint: can be computed for whole structure (*F*) or for each atomic site (*f*)

$$\Pi = \frac{1}{V^{1/3}} \int_0^\infty f^2 dR$$ **- Degree of order**

Local degree of order – indicates defects and low-symmetry sites

(e.g. for increased mutations)

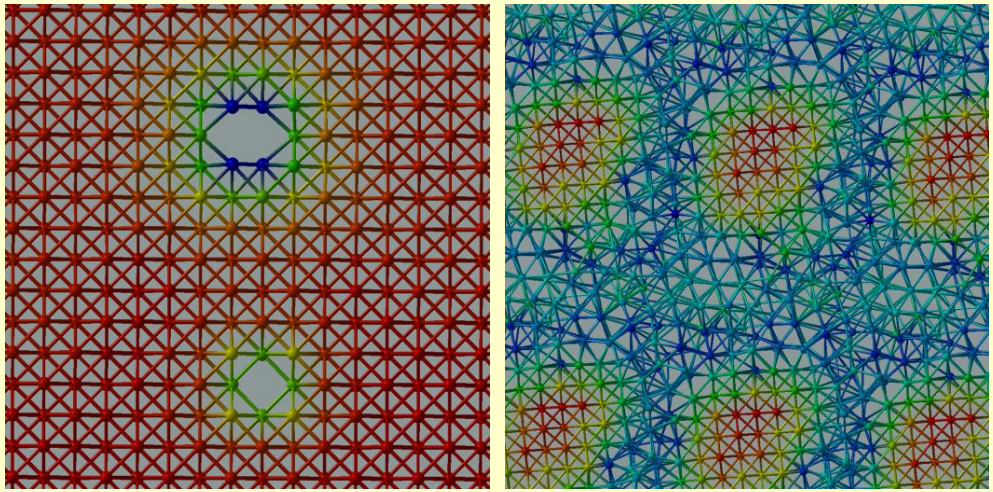

[Oganov & Valle (2009), Lyakhov et al. (2010)]

Without any empirical information, method reliably predicts materials

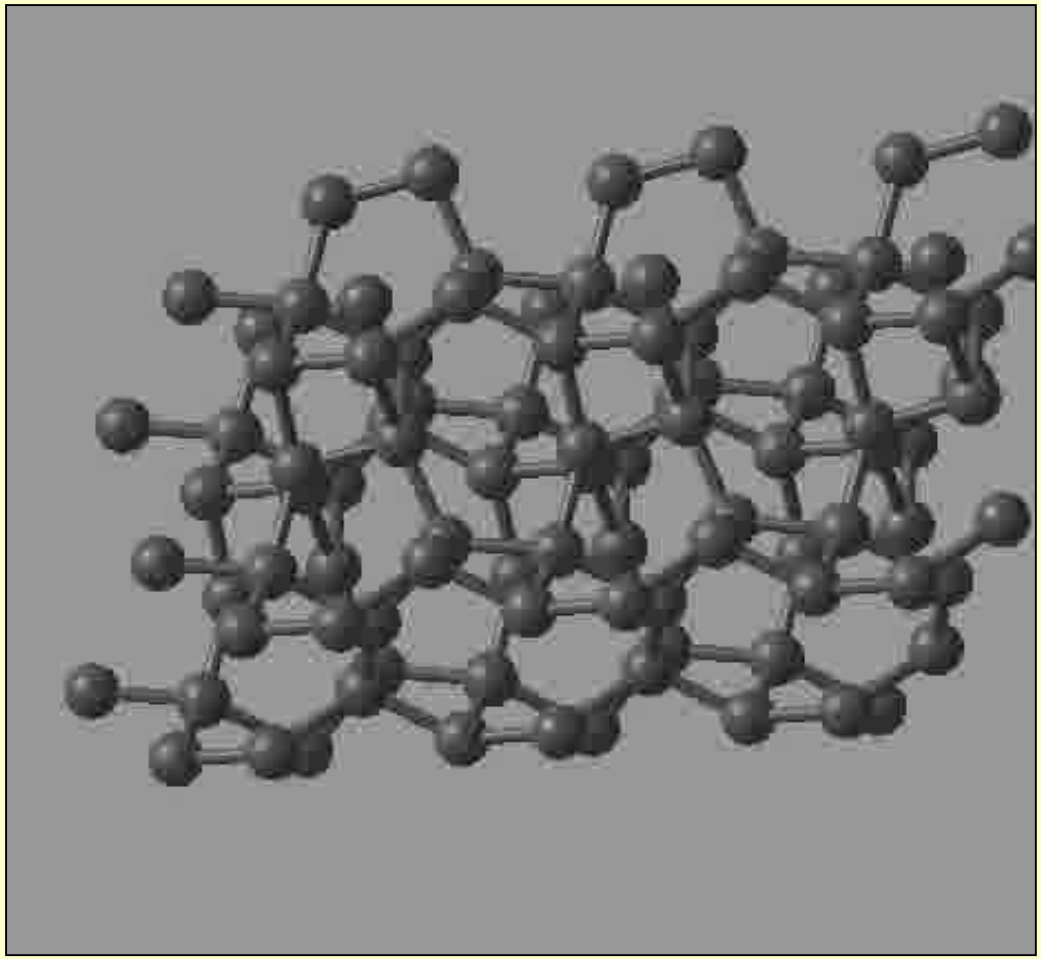

Carbon at 100 GPa – diamond structure is stable

The method is successful because of the topology of energy landscapes

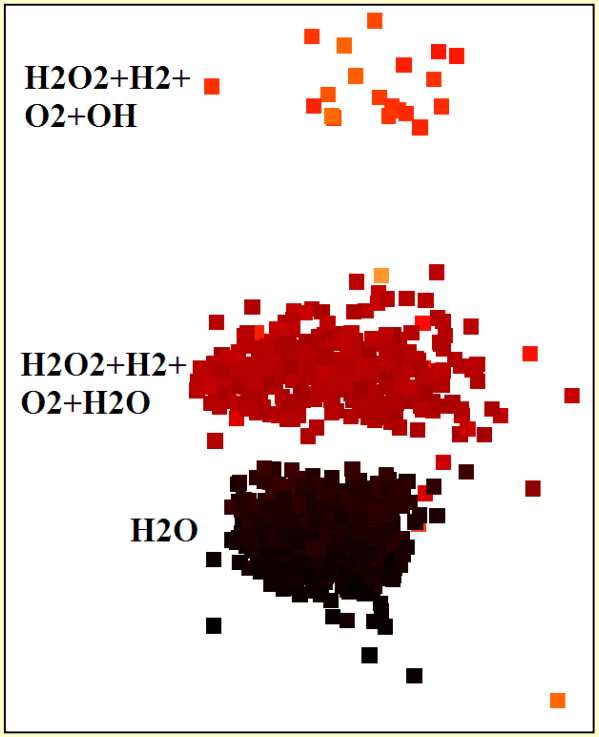

Distance-preserving mapping of crystal structures of H_2O (*darker* – lower E, *lighter* – higher E).

Au_8Pd_4 - simple

L_4J_8 - complex

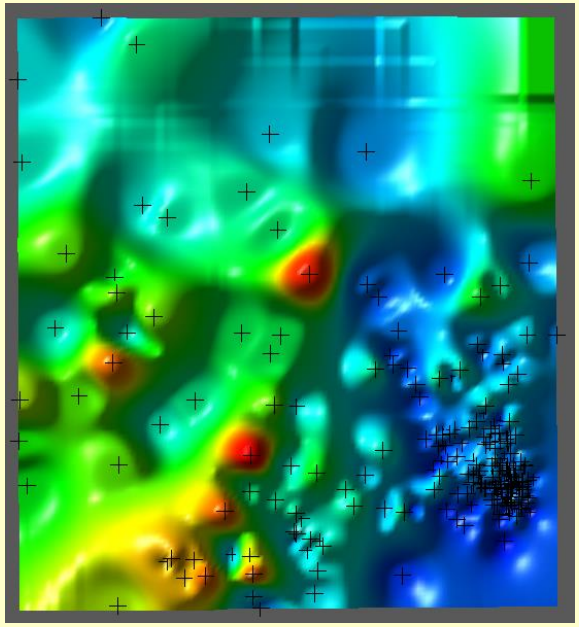

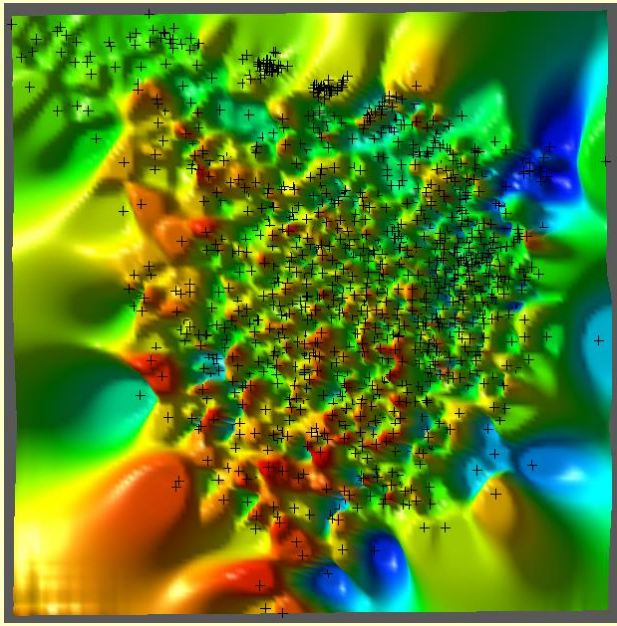

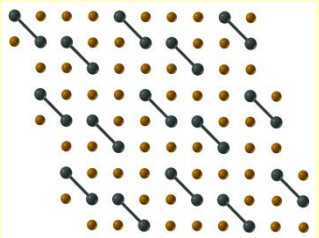

-61.960 eV

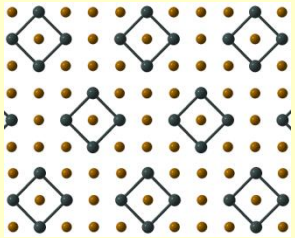

-61.957 eV

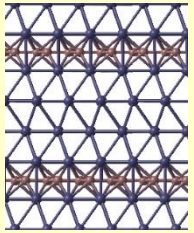

-99.12ε

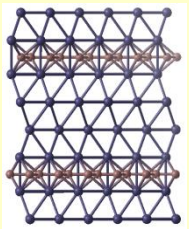

-99.05ε

[Oganov & Valle, *J. Chem. Phys.* 130, 104504 (2009)]

Why does USPEX work so well? A few tips and tricks

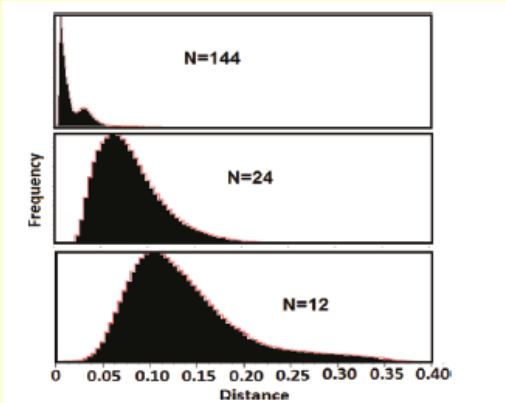

Distribution of distances between randomly sampled local minima in a binary Lennard-Jones system AB_2.

I. Reduction of dimensionality through unbiased symmetric initialization.

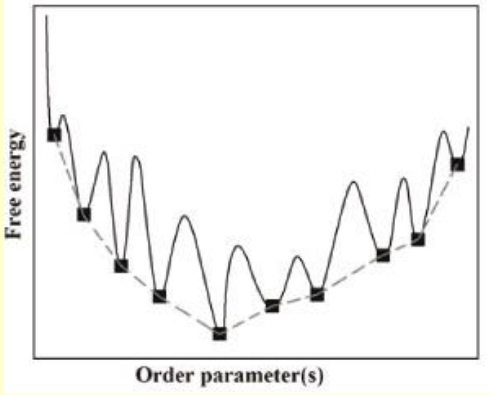

II. Reduction of effective dimensionality of problem by structure relaxation (also reduces "noise" and transforms energy landscape to a convenient shape).

formal dimensionality of full energy landscape: $d = 3N+3$

intrinsic dimensionality of reduced landscape: $d^* = 3N+3-\kappa$

number of distinct structures: $C^* \sim \exp(\beta d^*)$

$d^* = 10.9$ ($d = 39$) for Au_8Pd_4

$d^* = 11.6$ ($d = 99$) for $Mg_{16}O_{16}$

$d^* = 32.5$ ($d = 39$) for $Mg_4N_4H_4$

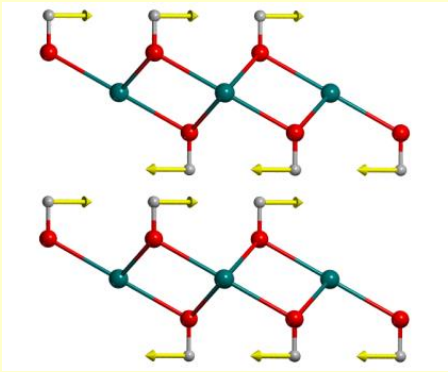

III. Variation operators are defined in subspaces of reduced dimensionality and involve cooperative transformations.

USPEX can automatically find all ground states in a multicomponent system.

Thermodynamic stability in variable-composition systems

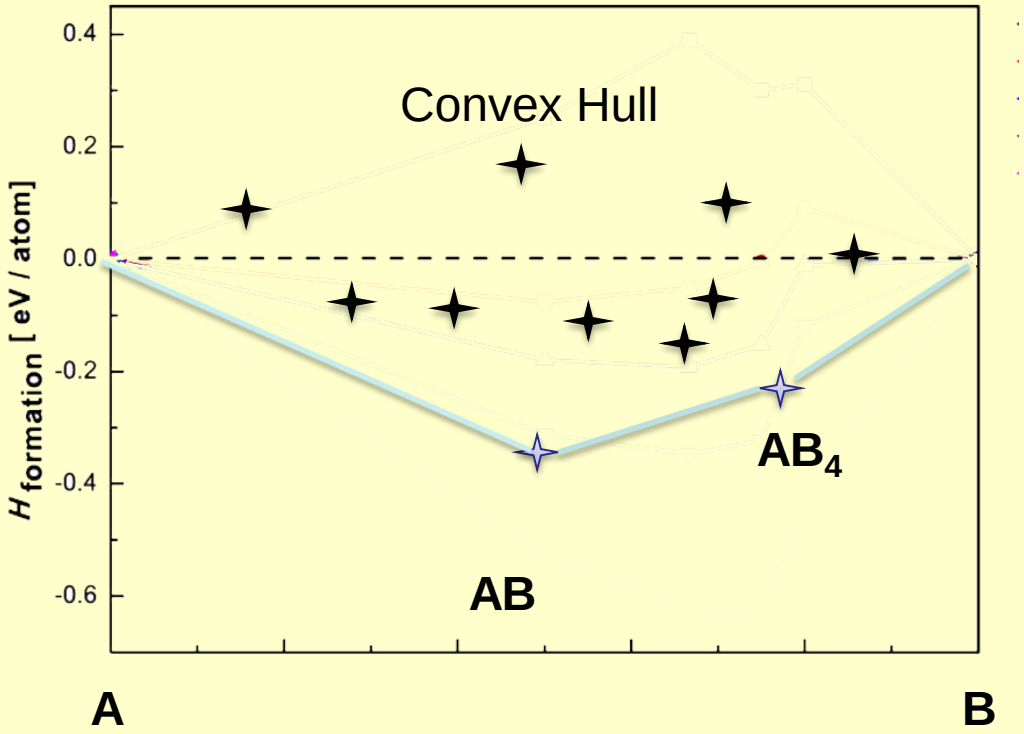

Stable structure must be below all the possible decomposition lines !!

Predicting “hidden” compounds (estimated 50% binaries, 99% ternaries)

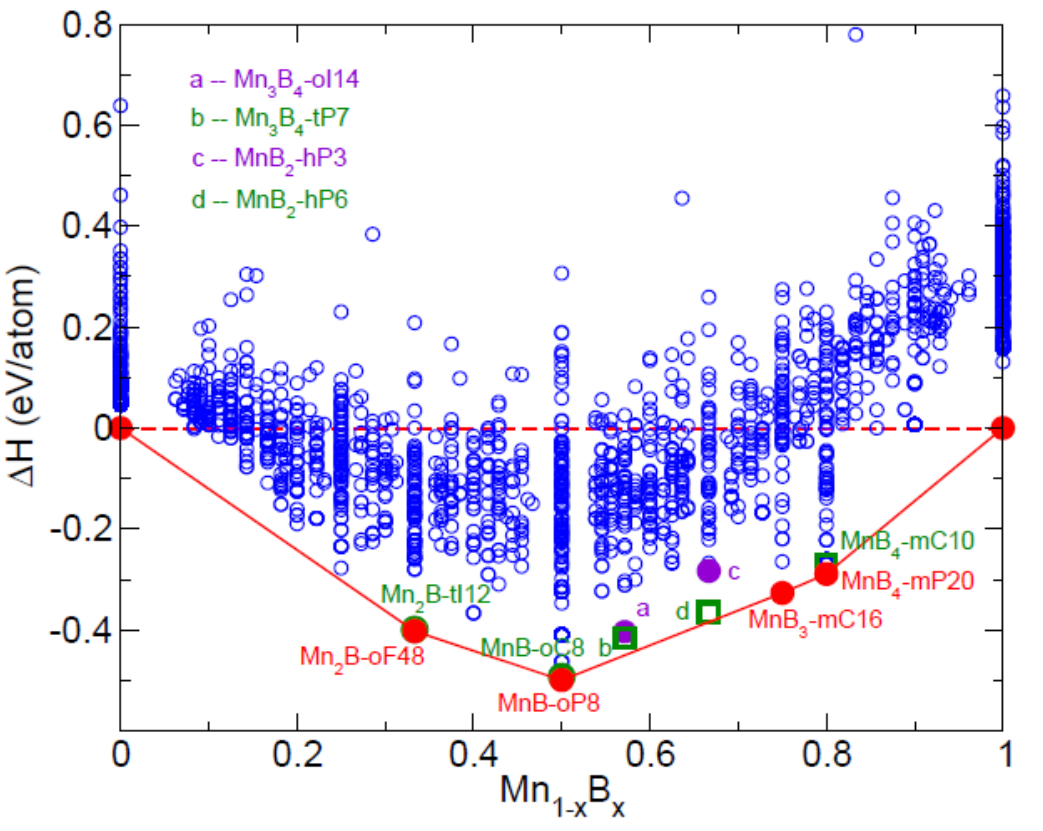

MnB3 was predicted and then synthesized (Niu, Chen, Oganov, et al., *PCCP* 2014)

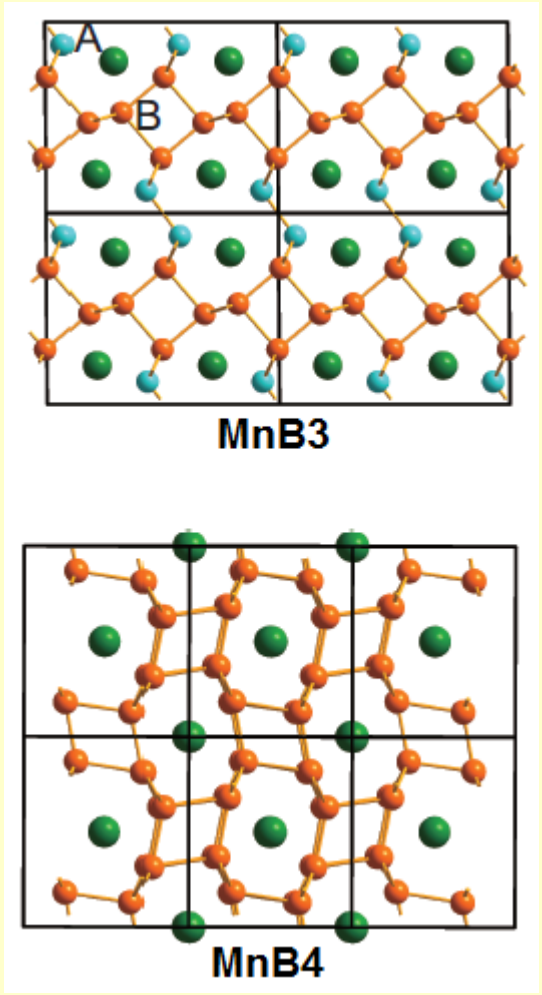

1. **New compound discovered – MnB_3.**
2. **For MnB_4, discovered the true structure, confirmed by later experiment.**

Can simultaneously optimize several properties – e.g. hardness and stability

Property optimization

- **Very few superhard systems (H > 40 GPa)**
- **Diamond is the hardest possible material**

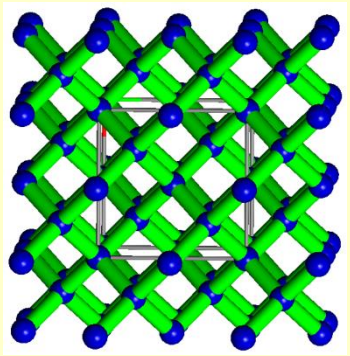

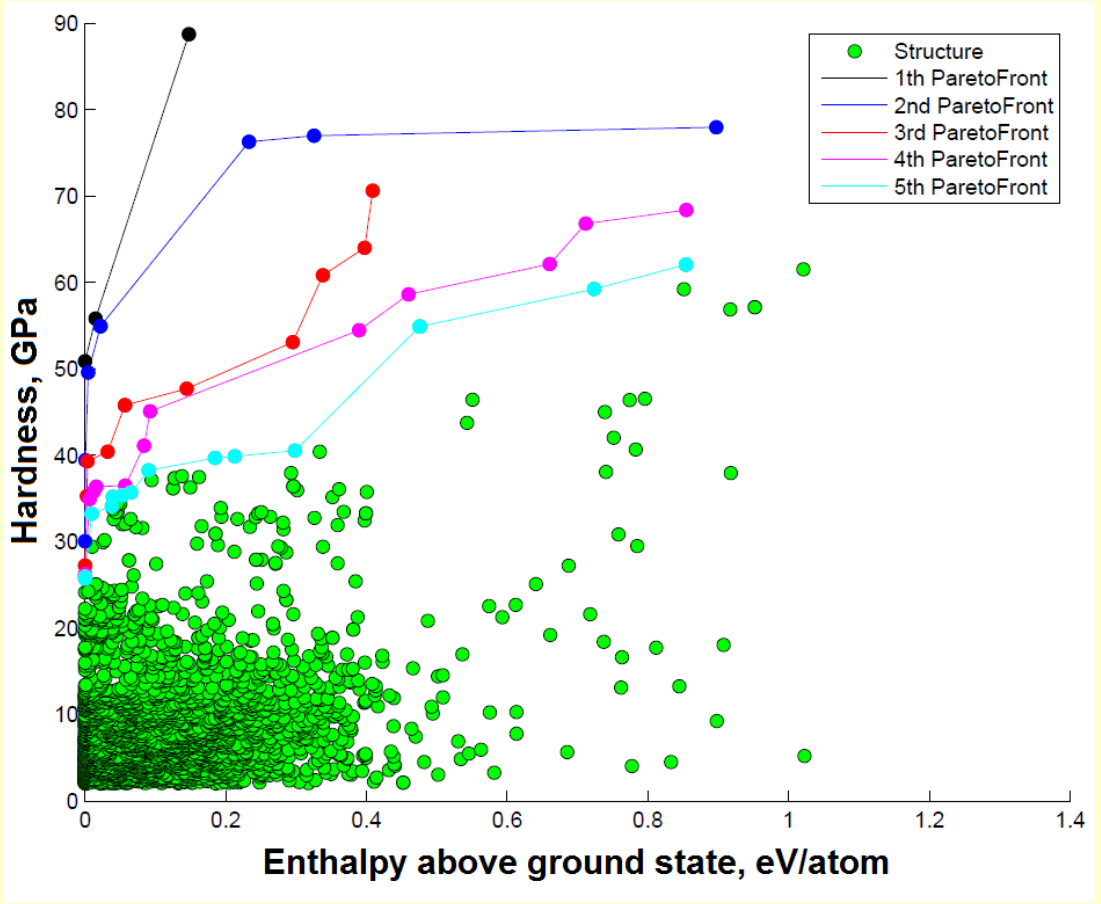

Adding different spin species and spin mutation operator, we simultaneously optimize composition, atomic and magnetic structure

Magnets

(1) Look at systems: HeavyMetal – MagneticMetal – (BindingElement) (e.g., W-Mn-B)
(2) For MagneticMetal, allow different magnetic moments.
(3) Add spin mutation operator.
(4) Among spin mutants, choose lowest-energy.
(5) Determine all stable compounds, see if any are ferromagnetic

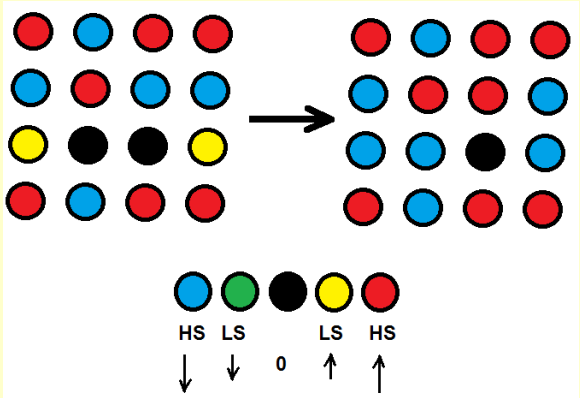

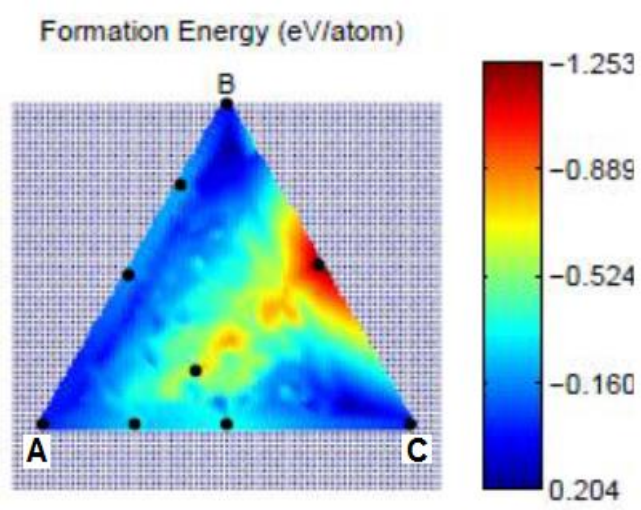

Composition	Enthalpy	Volume	Magmom	Magtype
[4 0 0]	-19.681	32.458	0.000	NM-LS
[0 16 0]	**-32.348**	**47.950**	**31.854**	**FM-HS**
[0 0 4]	-8.987	27.856	0.000	NM-NM
[2 14 0]	**-44.051**	**53.024**	**29.113**	**FM-HS**
[2 12 1]	-46.646	51.897	1.503	AFM-HS-LS
[4 0 8]	-41.926	85.496	0.000	NM-NM
[2 2 6]	-33.743	61.652	0.000	AFM-HS
[0 4 2]	-20.800	22.420	0.000	NM-NM

One of first designed magnets

Magnets

- $WMnB_2$ – one of the first examples of a purely theoretically designed material.
- Properties similar to Nd-based magnets, but ~2 times cheaper.
- Door to a new class of magnets.

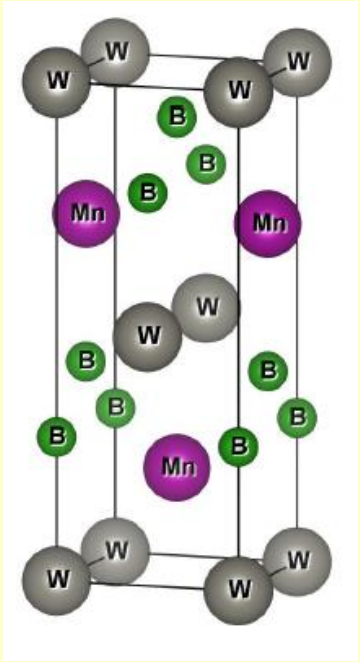

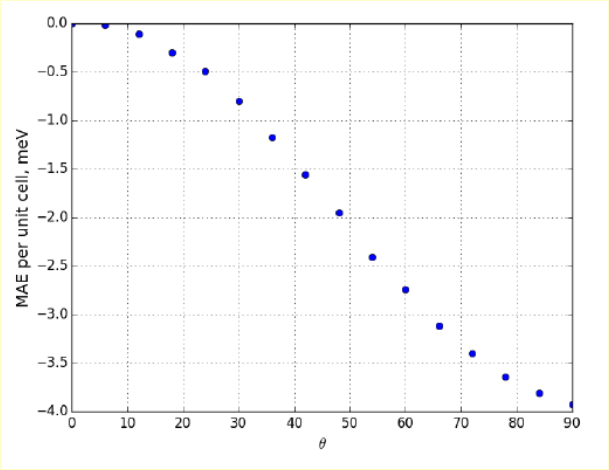

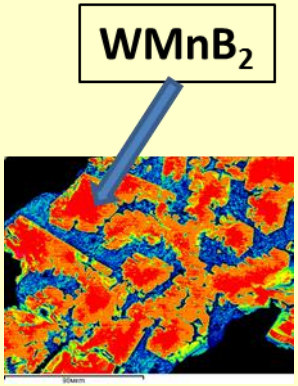

Magnetic moment and anisotropy of $Nd_2Fe_{14}B$ and predicted magnets

Material		Ms, $\mu_B/Å^3$	K1, MJ/m^3	K2, MJ/m^3
$WMnB_2$	[001]-[010]	**0.08**	**-5.2**	**0.41**
Mn_3Sn	[001]-[100]	**0.13**	**0.25**	**-0.23**
$Nd_2Fe_{14}B$	[001]-[010]	**0.13**	**6.5**	

Thermoelectrics: materials of the future

Thermoelectrics

Applications

Water/Beer/Wine Cooler

www.kingsbottle.com

Cooled Car Seat

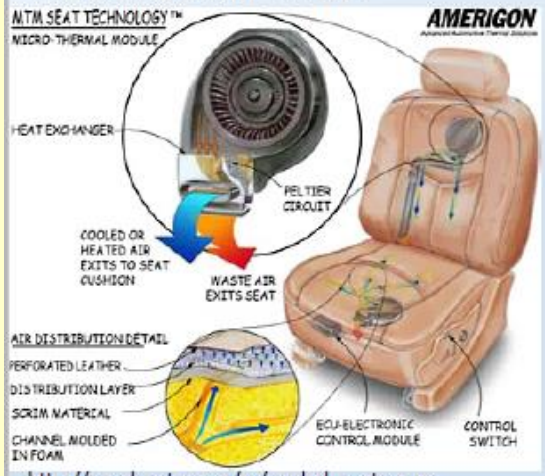

http://wardsauto.com/ar/cooled_seats_mpg

Laser/OE Cooling

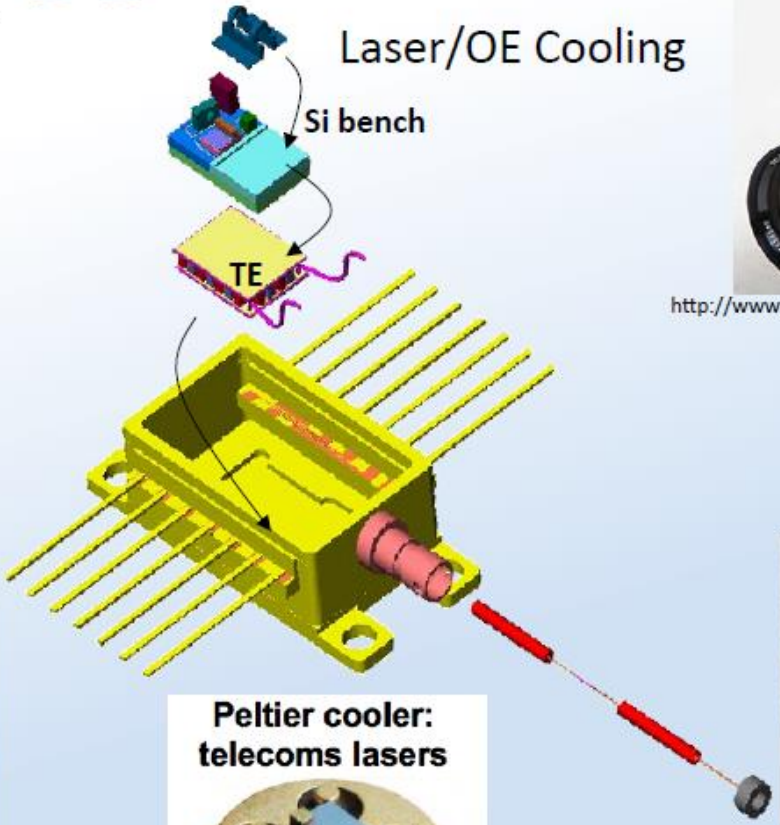

Peltier cooler: telecoms lasers

Copyright Micropelt

Cryogenic IR Night Vision

http://www.x20.org/products/pv400-used-night-vision-scope/

Electronic Cooling

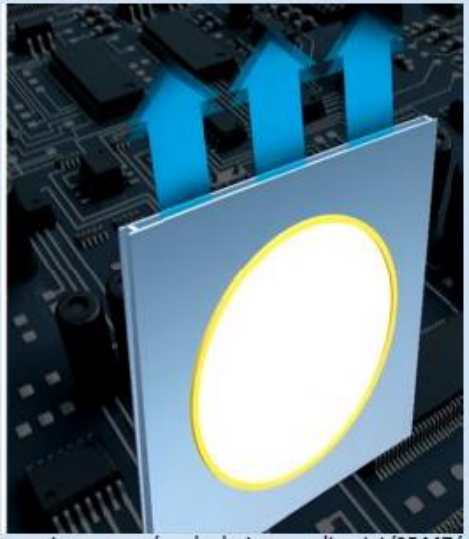

http://www.gizmag.com/ge-dual-piezo-cooling-jet/25447/

Test: simultaneous optimization of ZT and *E* found the known and a new thermoelectric polymorph of Bi_2Te_3

Thermoelectrics

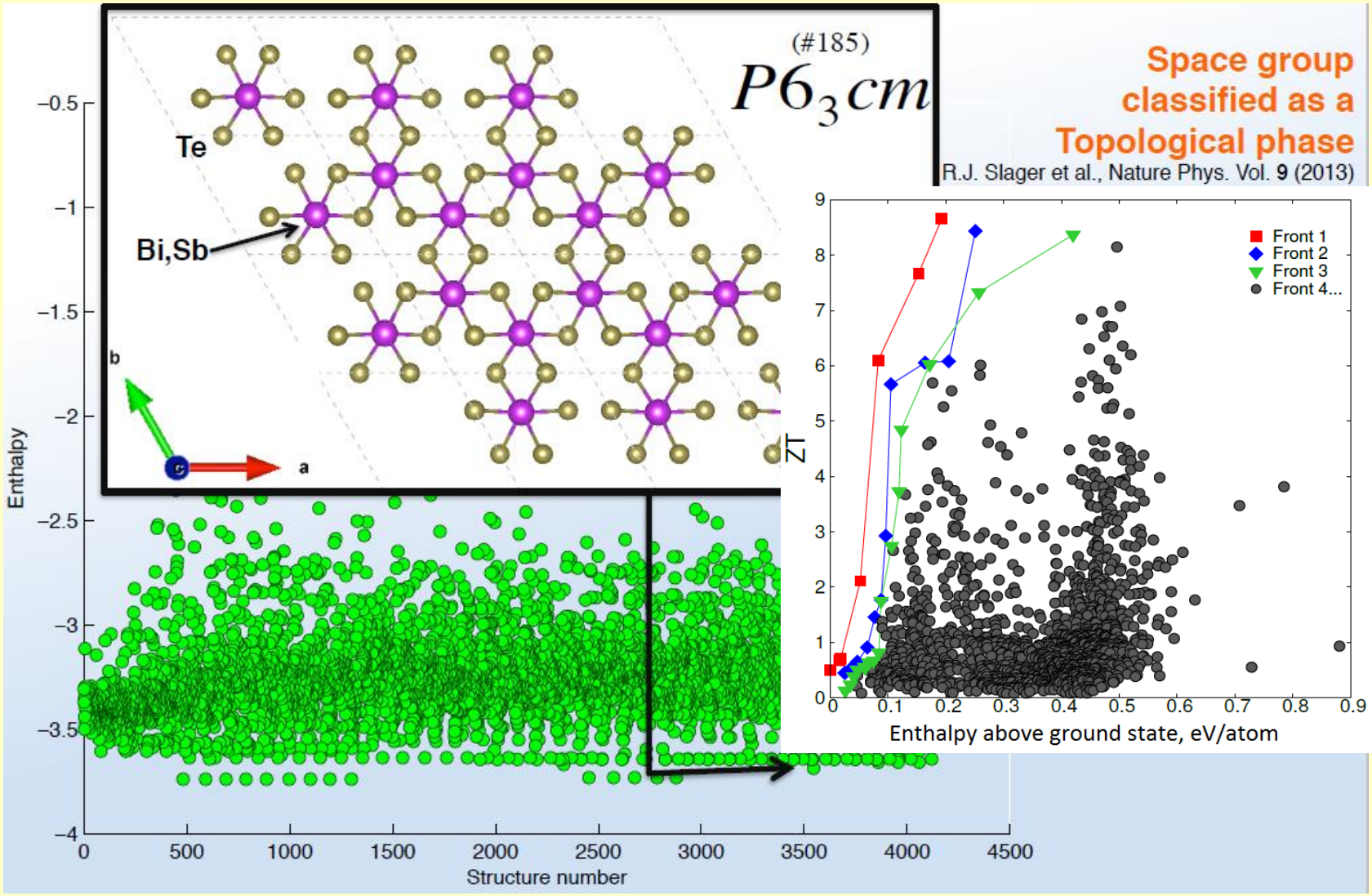

II. Predicting new materials and phenomena

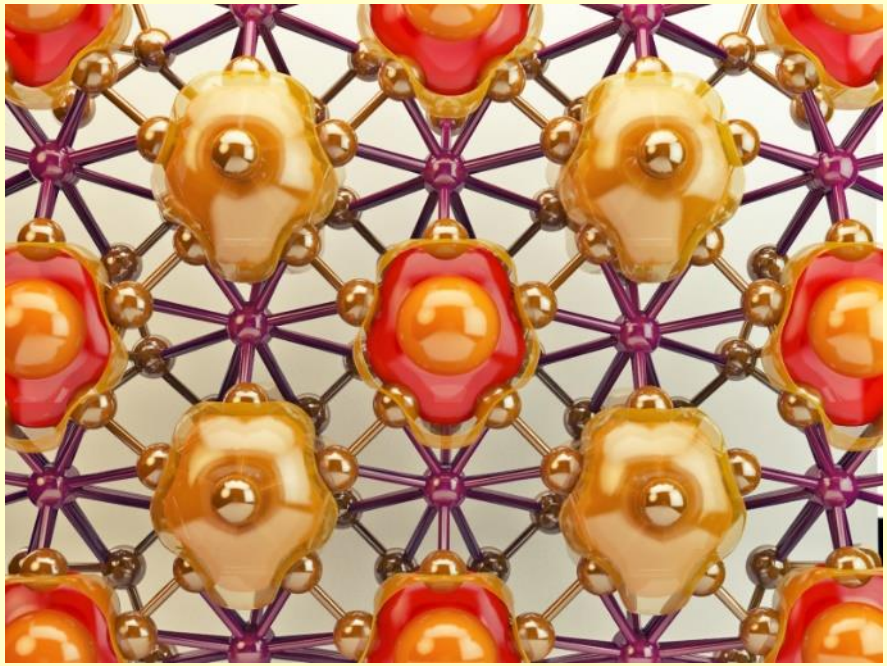

New superhard structure of boron
(Oganov et al., *Nature*, 2009)

High-pressure transparent allotrope of sodium
(Ma, Eremets, Oganov, *Nature*, 2009)

Na-Cl

Predictive power of modern methods:

Na_3Cl, Na_2Cl, Na_3Cl_2, NaCl, $NaCl_3$, $NaCl_7$ are stable under pressure (Zhang, Oganov, et al. *Science*, 2013).

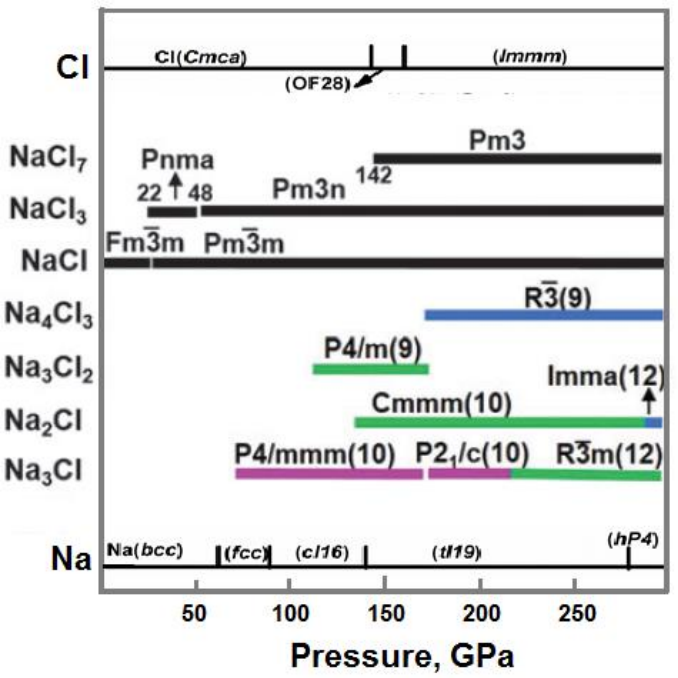

Stability fields of sodium chlorides

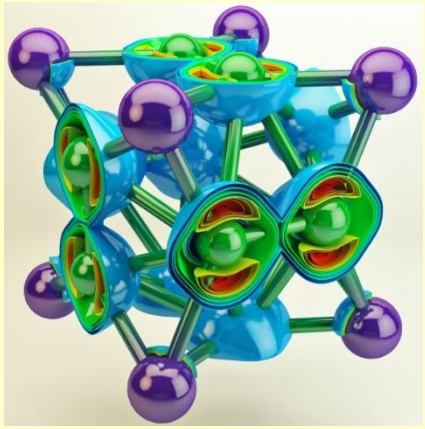

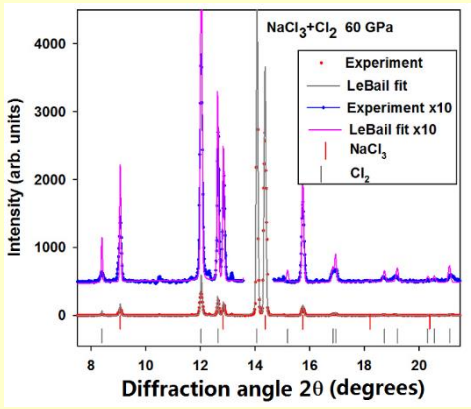

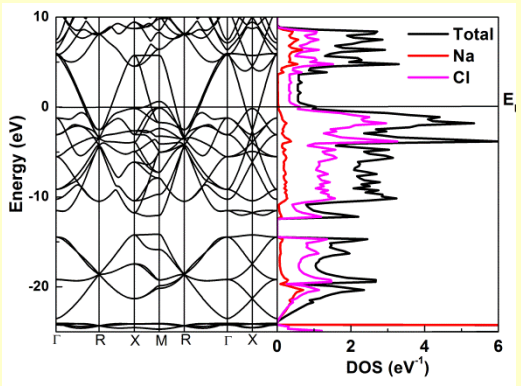

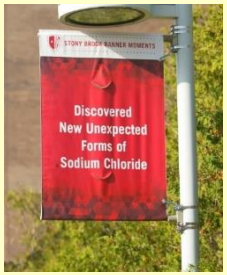

$NaCl_3$: atomic and electronic structure, and experimental XRD pattern

Chemical anomalies:

-Divalent Cl in Na_2Cl!
-Coexistence of metallic and ionic blocks in Na_3Cl!
-Positively charged Cl in $NaCl_7$!

[Zhang, Oganov, et al., *Science* (2013)]
[Saleh & Oganov, *PCCP* (2015)]

K-Cl: extreme richness of the phase diagram

(Zhang, Oganov, Goncharov, 2016). Predictions confirmed by experiment!

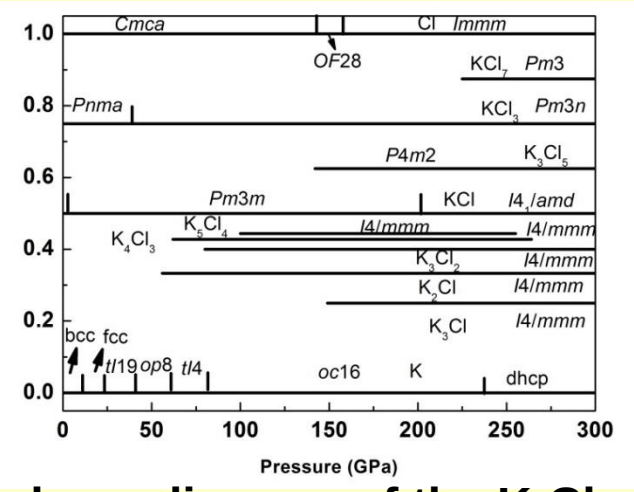

P-x phase diagram of the K-Cl system

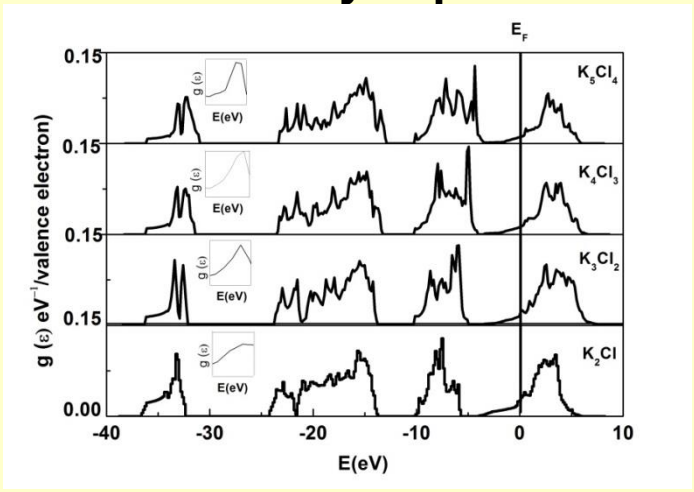

Electronic DOS of K-Cl compounds

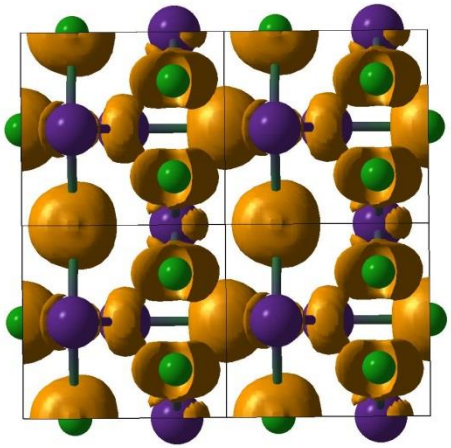

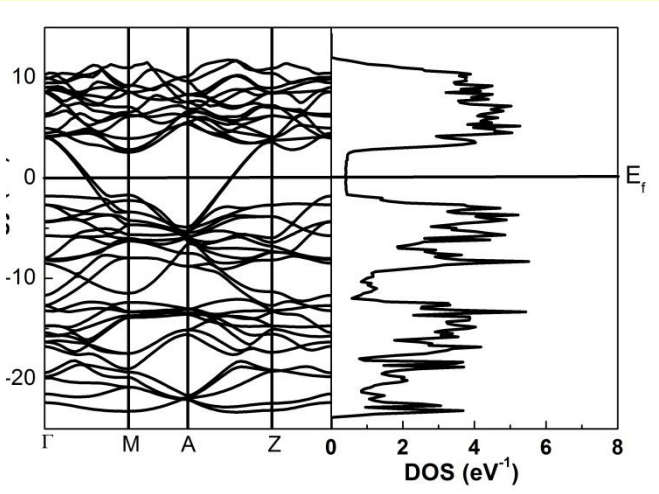

Electronic structure of K_3Cl_5

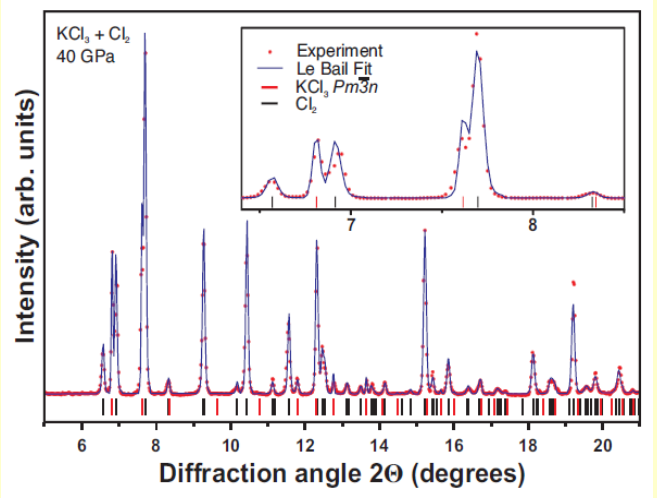

Experimental X-ray diffraction of KCl_3

Ca-C

Ca-C system: path to new hydrocarbons

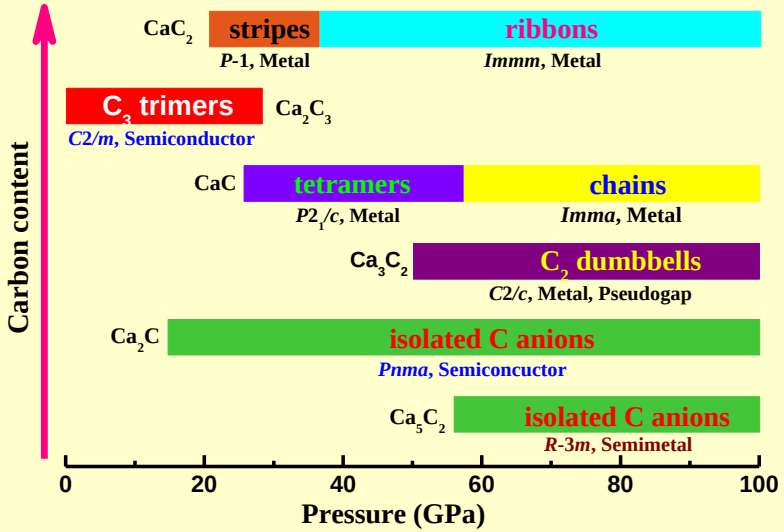

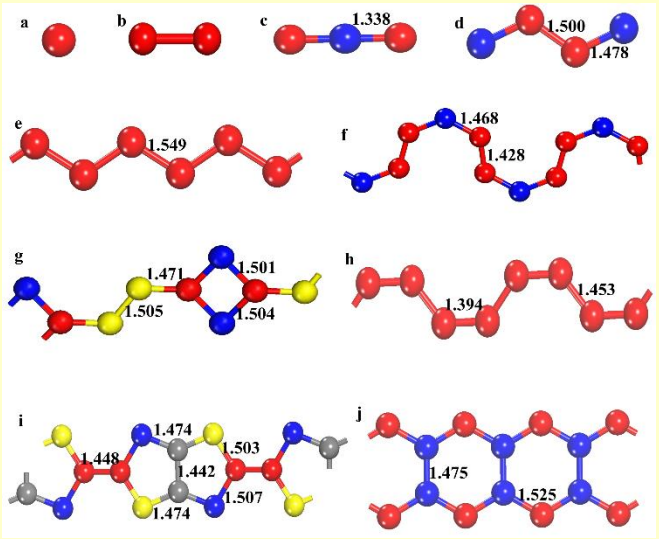

Chemical phase diagram of the Ca-C system

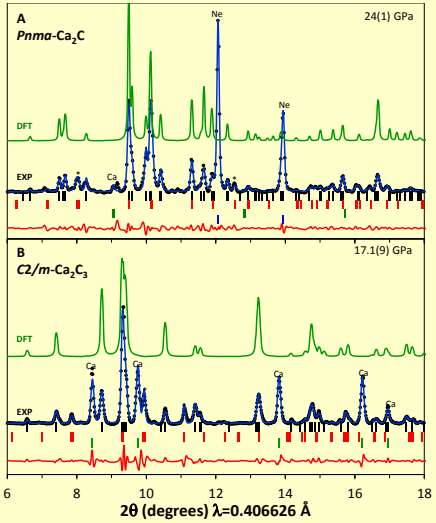

Experimental confirmation of Ca_2C and Ca_2C_3.
Mg_2C_3 contains rare allylenide-ion. Hydrolysis yields propyne C_3H_4.

[Li & Oganov, *Nature Communications*, 2015]

Extended concept of electronegativity to explain new compounds

Dong & Oganov (2015): extended electronegativity and chemical hardness to arbitrary pressures.

Mulliken electronegativity $dE/dN\big|_{N=0} = \mu = -\chi$

chemical hardness $\eta = c = \frac{1}{2} d^2E/dN^2\big|_{N=0}$

Ni becomes "noble gas-like" insulator at 34 TPa (McMahah, 1982).

Na, Mg, Cu more reactive under pressure.

Fe and Co become acceptors of electrons.

MgFe should become stable. Indeed the case.

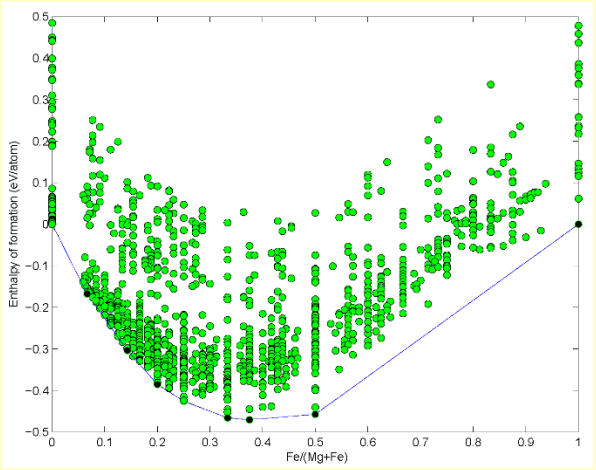

Thermodynamics of Mg-Fe system at 200 GPa

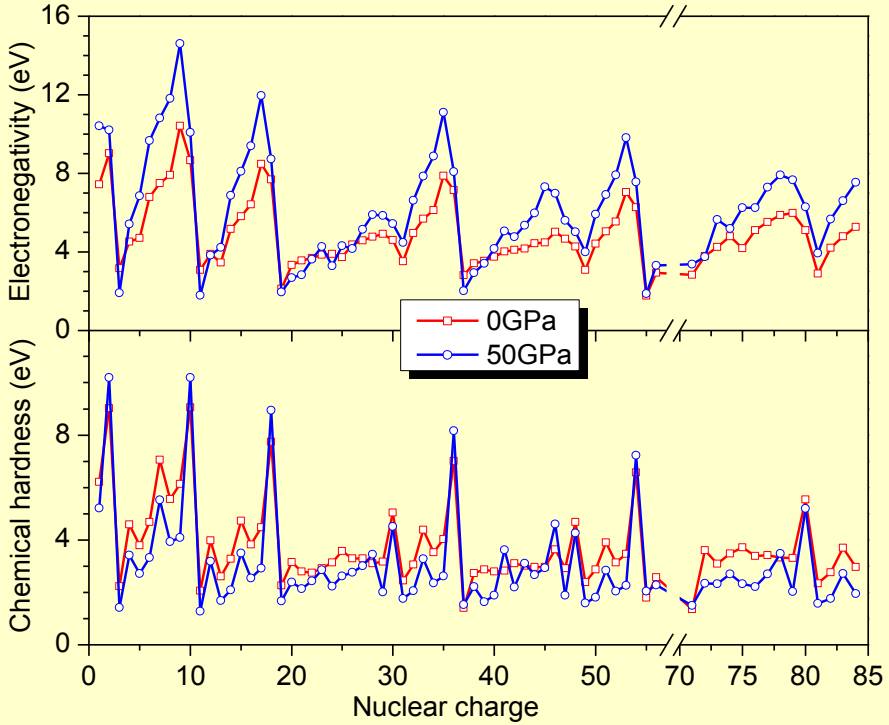

Electronegativities and chemical hardnesses of the elements (Dong & Oganov, 2015)

«Forbidden» compounds can exist in planetary interiors

(1) Rocky planets
(Mercury, Venus, Mars, Earth):

-Relatively small
-Solid
-Mantle – crudely, $MgSiO_3$
-Core – Fe with impurities (~20 мол.%)
-Earth's center – 364 GPa, 6000 K.

(2) Gas giants:

-Large
-Fluid
-Composition:
Jupiter, Saturn - H+He
Uranus, Neptune – H_2O+CH_4+NH_3
-Jovian center – 50000 GPa (?), 24000 K (?).

(3,4,...) Exoplanets: gas giants, superearths, diamond planets

Super-Earths

"Forbidden" MgO_2, Mg_3O_2, SiO, SiO_3 are stable at planetary pressures

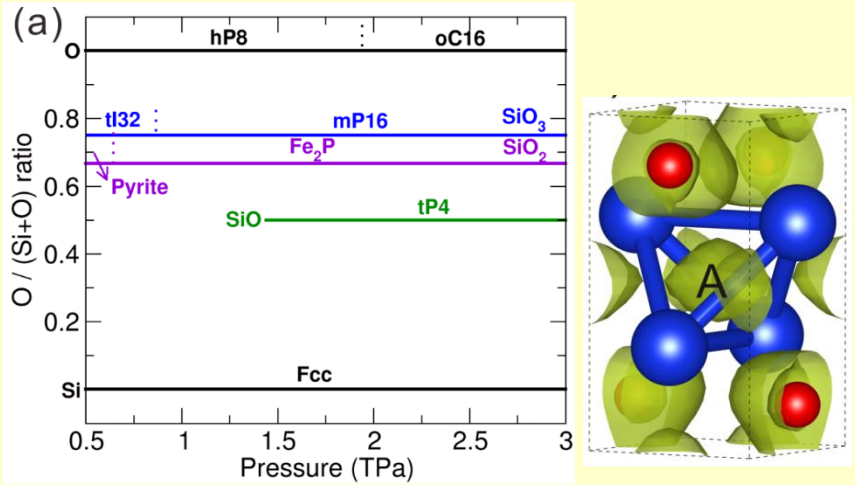

Phase diagram of Si-O system and structure of SiO (Niu & Oganov, 2015)

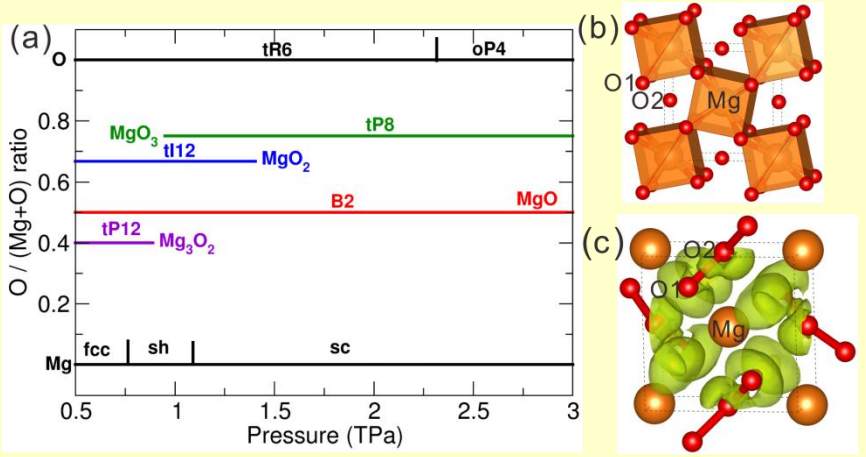

Phase diagram of Mg-O system and structure of MgO_3 (Niu & Oganov, 2015; Zhu & Oganov, 2013)

Experiment:
[Lobanov S. et al., *Sci. Rep.* 5, 13582 (2015)].

Niu H., Oganov A.R., Chen X., Li D., *Sci. Rep.* 5, 18347 (2015).
Zhu Q., Oganov A.R., Lyakhov A.O., *Phys. Chem. Chem. Phys.* 15, 7796-7700 (2013).

Super-Earths

At ultrahigh pressures $MgSiO_3$ post-perovskite decomposes

$$MgSiO_3 \rightarrow Mg_2SiO_4 + MgSi_2O_5 \rightarrow Mg_2SiO_4 + SiO_2 \rightarrow MgO + SiO_2 \ (T < 6500\ K)$$

$$MgSiO_3 \rightarrow Mg_2SiO_4 + MgSi_2O_5 \rightarrow MgSi_2O_5 + MgO \rightarrow MgO + SiO_2 \ (T > 6500\ K)$$

Multistage decomposition implies complex structure of super-Earths
[Niu H., Oganov A.R., Chen X., Li D., *Sci. Rep.* 5, 18347 (2015)].

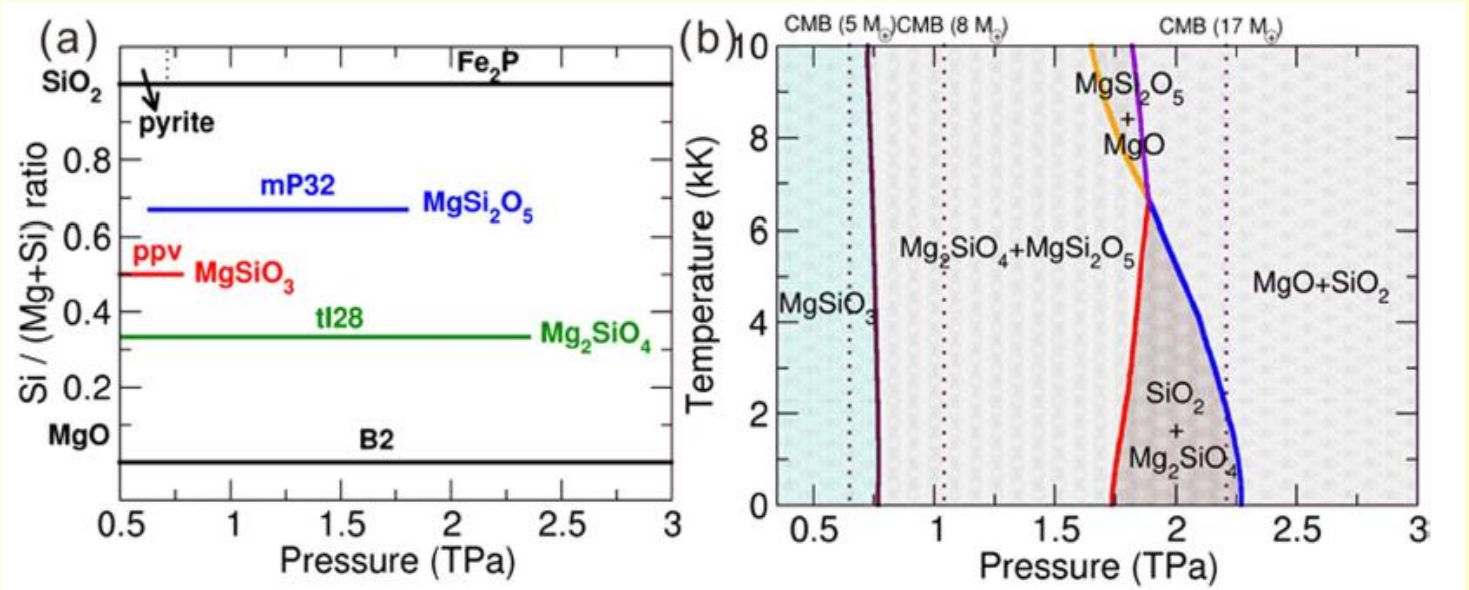

Figure 4. (a) Pressure-composition phase diagram of the pseudo-binary MgO-SiO_2 system. (b) *P-T* phase diagram of $MgSiO_3$. The core-mantle boundary (CMB) pressures of super-Earths and mega-Earths with 5, 8 and 17 $M_\oplus$ are also plotted by vertical dashed lines.

“Forbidden” $MgSi_3O_{12}$ and $MgSiO_6$ are stable at pressures of mantles of super-Earths

Super-Earths

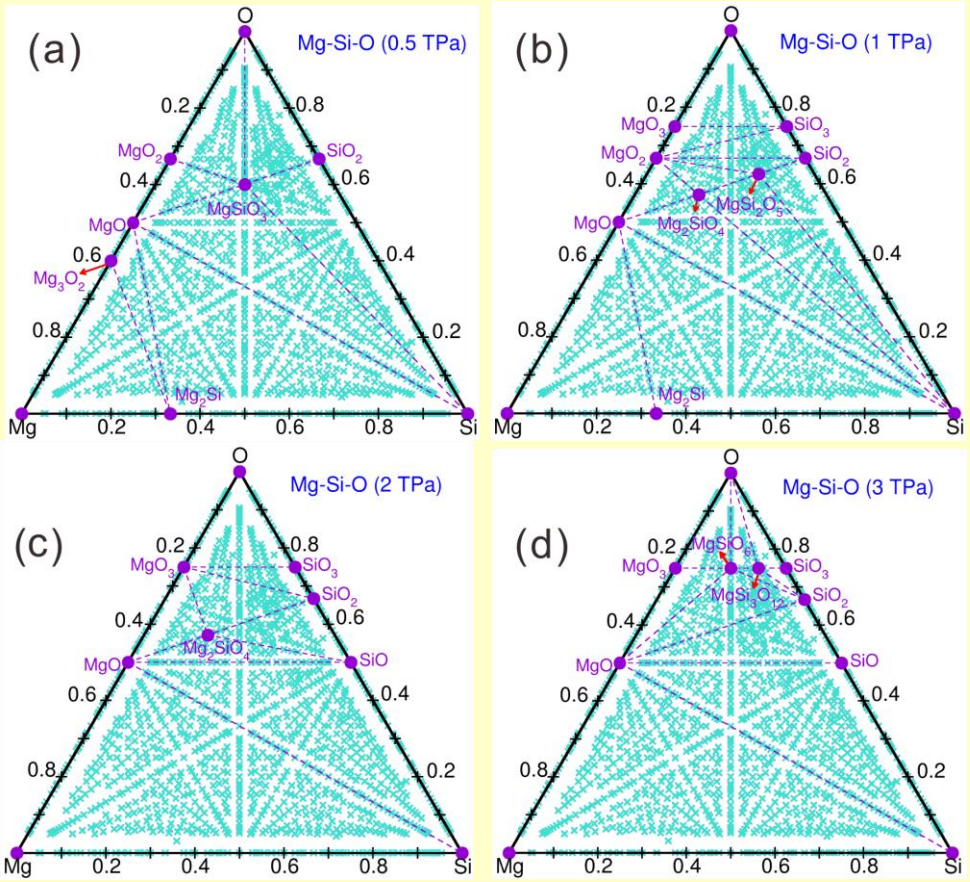

Phase diagram of Mg-Si-O system [Niu H., Oganov A.R., Chen X., Li D., *Sci. Rep.* 5, 18347 (2015)].

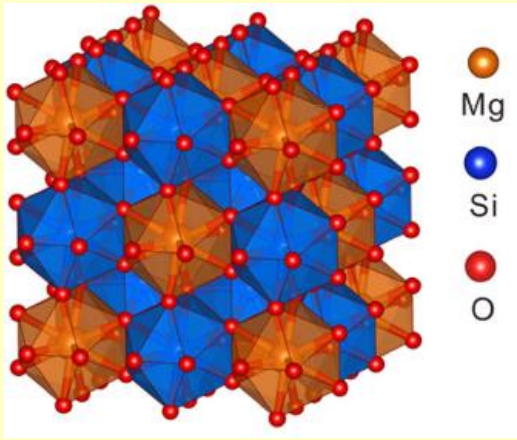

Structure of $MgSi_3O_{12}$

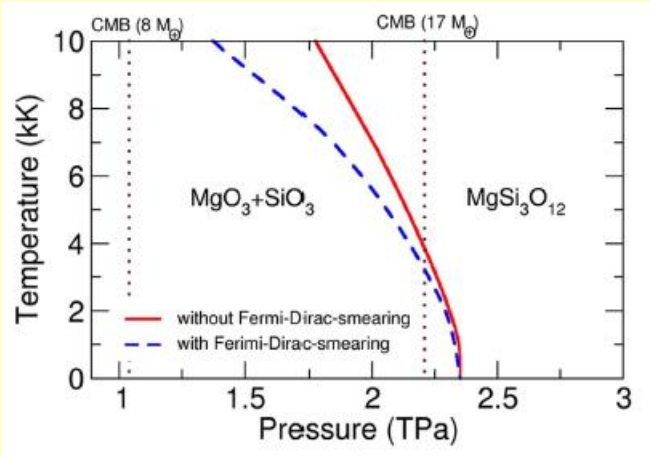

Phase diagram of $MgSi_3O_{12}$

Uranus, Neptune

C-H-O system under pressure

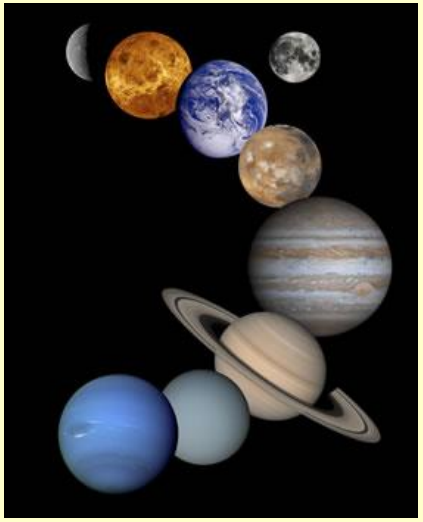

- Uranus and Neptune: $H_2O:CH_4:NH_3$ = 59:33:8.
- Temperature in the center – 5500 K, pressure – 800 GPa.

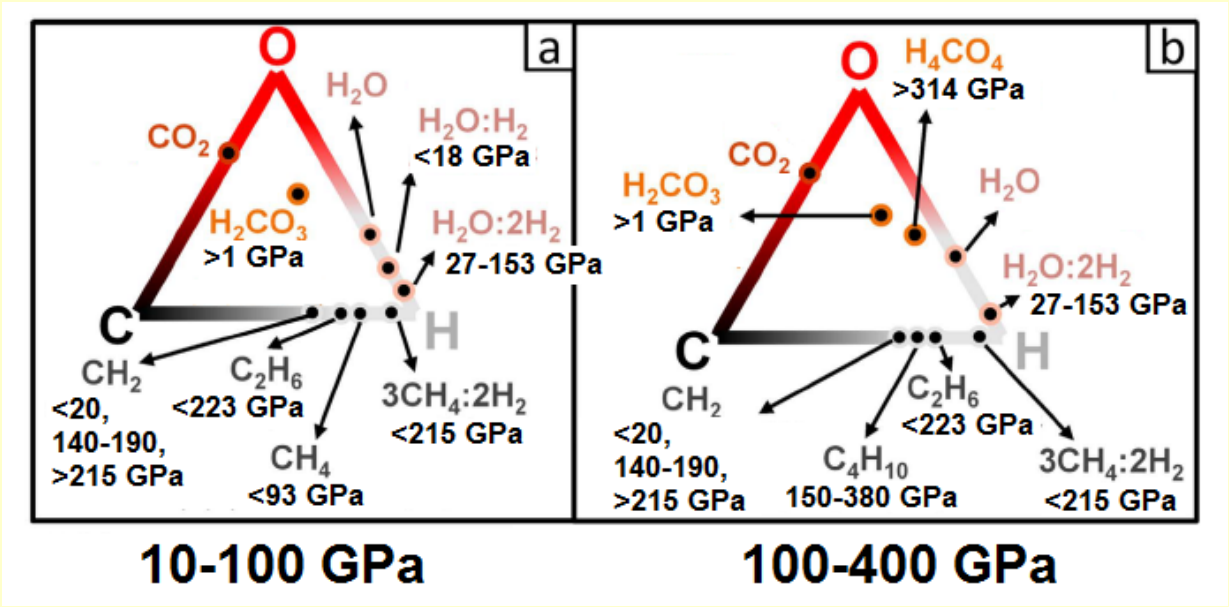

- Ice H_2O and CO_2 are stable at all pressures.
- Methane CH_4: decomposes above 93 GPa. Ethane, butane, polyethylene stable.
- Carbonic acid H_2CO_3 stable at >1 GPa polymeric at >44 GPa.

Experimental confirmation: Wang H., et al., *Sci. Rep.* 6, 19902 (2016).

- Orthocarbonic acid H_4CO_4 is stable at >314 GPa.

[Saleh G., Oganov A.R, *Sci. Rep.* 6, 32486 (2016)]

High-pressure hydronitrogens (Qian, Oganov, 2016)

Uranus, Neptune

- Polymeric hydronitrogens
  - N_xH $(x \geq 1)$
- 2D-polymeric phase
  - N_9H_4
- Molecular hydronitrogens
  - NH_5, NH_4, NH_3, NH_2, N_3H_7
  - N_8H

Green: molecular

Purple: molecular ionic

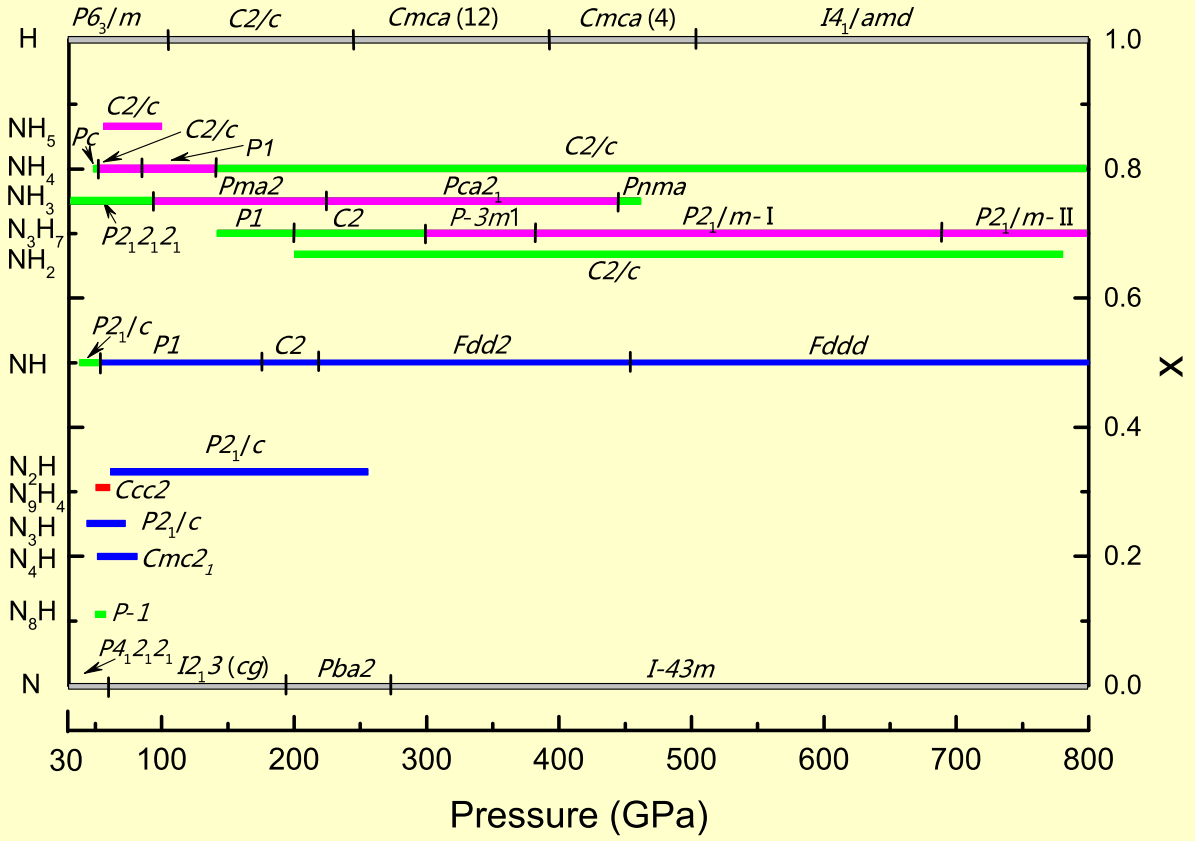

Uranus, Neptune

Hydronitrogen at ambient pressure

NH_3 (ammonia)

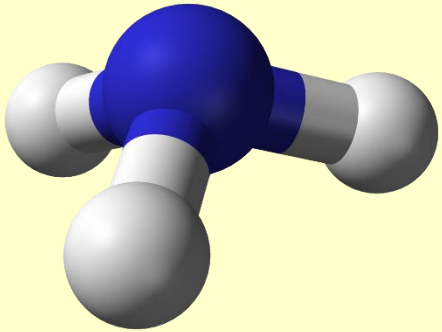

N_5H (pentazole)

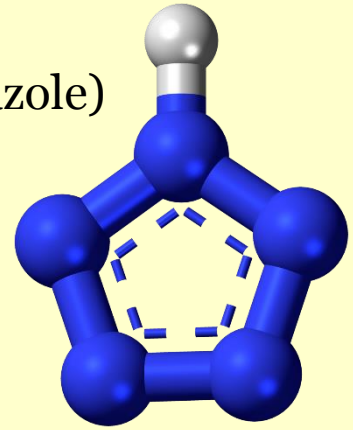

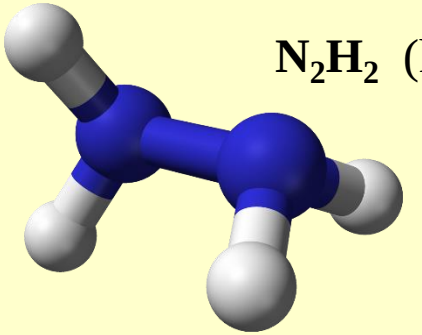

N_2H_2 (hydrazine)

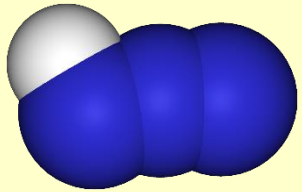

HN_3 (hydrazoic acid)

High-pressure hydronitrogens

Uranus, Neptune

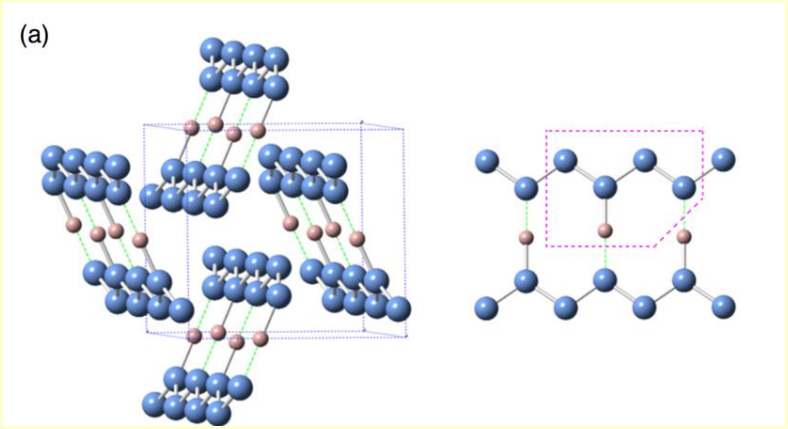

N_4H

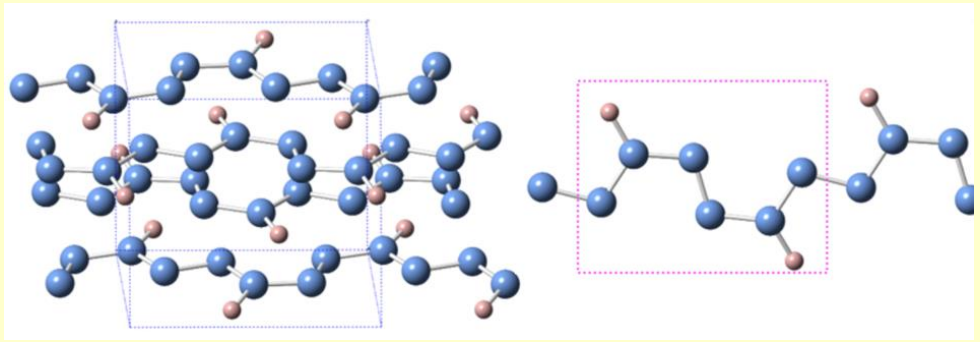

N_3H

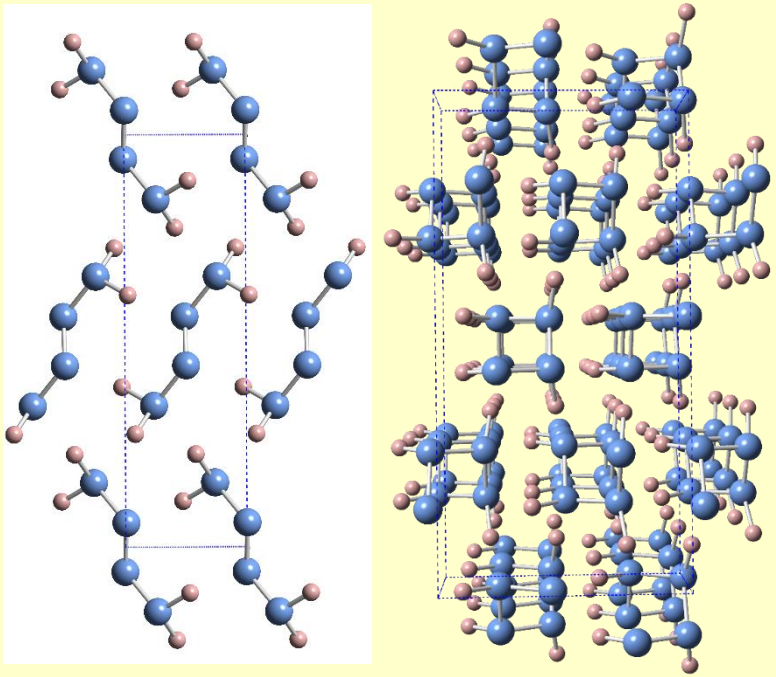

NH

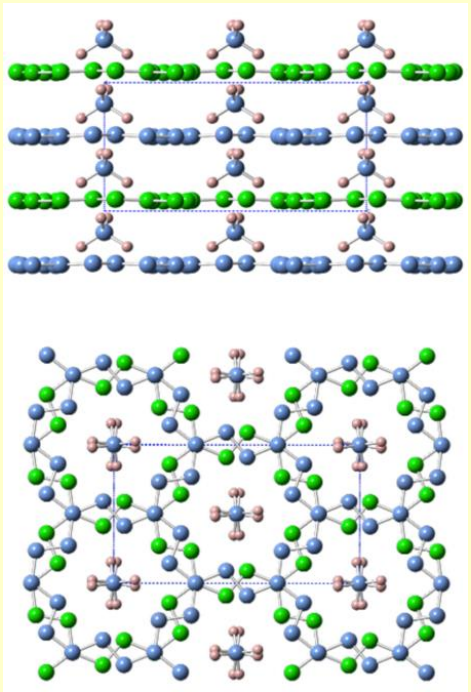

N_4H_9

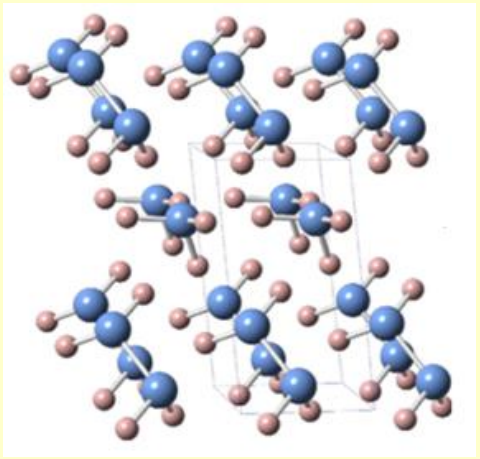

N_3H_7

Highest-Tc superconductivity: new record, 203 Kelvin

H-S

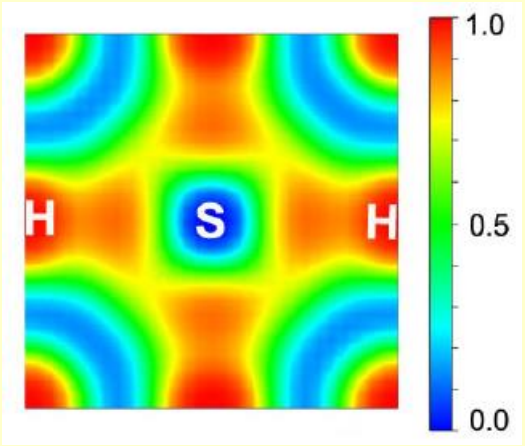

OPEN

SUBJECT AREAS:
THEORY AND COMPUTATION
CONDENSED MATTER PHYSICS

Received
7 July 2014

Accepted
29 September 2014

Published
10 November 2014

Correspondence and requests for materials should be addressed to T.C. (cuitian@jlu.edu.cn)

Pressure-induced metallization of dense $(H_2S)_2H_2$ with high-T_c superconductivity

Defang Duan[1,2], Yunxian Liu[1], Fubo Tian[1], Da Li[1], Xiaoli Huang[1], Zhonglong Zhao[1], Hongyu Yu[1], Bingbing Liu[1], Wenjing Tian[2] & Tian Cui[1]

[1]State Key Laboratory of Superhard Materials, College of physics, Jilin University, Changchun, 130012, P. R. China, [2]State Key Laboratory of Supramolecular Structure and Materials, Jilin University, Changchun, 130012, P. R. China.

The high pressure structures, metallization, and superconductivity of recently synthesized H_2-containing compounds $(H_2S)_2H_2$ are elucidated by *ab initio* calculations. The ordered crystal structure with *P*1 symmetry is determined, supported by the good agreement between theoretical and experimental X-ray diffraction data, equation of states, and Raman spectra. The *Cccm* structure is favorable with partial hydrogen bond symmetrization above 37 GPa. Upon further compression, H_2 molecules disappear and two intriguing metallic structures with *R*3*m* and *Im*-3*m* symmetries are reconstructive above 111 and 180 GPa, respectively. The predicted metallization pressure is 111 GPa, which is approximately one-third of the currently suggested metallization pressure of bulk molecular hydrogen. Application of the Allen-Dynes-modified McMillan equation for the *Im*-3*m* structure yields high T_c values of 191 K to 204 K at 200 GPa, which is among the highest values reported for H_2-rich van der Waals compounds and MH_3 type hydride thus far.

Conventional superconductivity at 203 kelvin at high pressures in the sulfur hydride system

A. P. Drozdov, M. I. Eremets, I. A. Troyan, V. Ksenofontov & S. I. Shylin

Nature (2015) | doi:10.1038/nature14964
Received 25 June 2015 | Accepted 22 July 2015 | Published online 17 August 2015

A superconductor is a material that can conduct electricity without resistance below a superconducting transition temperature, T_c. The highest T_c that has been achieved to date is in the copper oxide system[1]: 133 kelvin at ambient pressure[2] and 164 kelvin at high pressures[3]. As the nature of superconductivity in these materials is still not fully understood (they are not conventional superconductors), the prospects for achieving still higher transition temperatures by this route are not clear. In contrast, the Bardeen–Cooper–Schrieffer theory of conventional superconductivity gives a guide for achieving high T_c with no theoretical upper bound—all that is needed is a favourable combination of high-frequency phonons, strong electron–phonon coupling, and a high density of states[4]. These conditions can in principle be fulfilled for metallic hydrogen and covalent compounds dominated by hydrogen[5, 6], as hydrogen atoms provide the necessary high-frequency phonon modes as well as the strong electron–phonon coupling. Numerous calculations support this idea and have predicted transition temperatures in the range 50–235 kelvin for many hydrides[7], but only a moderate T_c of 17 kelvin has been observed experimentally[8]. Here we investigate sulfur hydride[9], where a T_c of 80 kelvin has been predicted[10]. We find that this system transforms to a metal at a pressure of approximately 90 gigapascals. On cooling, we see signatures of superconductivity: a sharp drop of the resistivity to zero and a decrease of the transition temperature with magnetic field, with magnetic susceptibility measurements confirming a T_c of 203 kelvin. Moreover, a pronounced isotope shift of T_c in sulfur deuteride is suggestive of an electron–phonon mechanism of superconductivity that is consistent with the Bardeen–Cooper–Schrieffer scenario. We argue that the phase responsible for high-T_c superconductivity in this system is likely to be H_3S, formed from H_2S by decomposition under pressure. These findings raise hope for the prospects for achieving room-temperature superconductivity in other hydrogen-based materials.

Prior record Tc=135 K (Putilin, Antipov, 1993) is broken: theorists (T. Cui, 2014) predicted new compound H_3S with Tc~200 K. Confirmed by A.Drozdov (Nature, 2015).

Remarkable superconductivity of “forbidden” compounds

$$T_c = \frac{\omega_{\log}}{1.2}\exp\left[-\frac{1.04(1+\lambda)}{\lambda-\mu^*(1+0.62\lambda)}\right]$$

- **Pure metallic hydrogen: Tc=242 K at 450 K (Cudazzo, 2008).**
- **LiH_6 (discovered by Zurek, Hoffmann & Oganov, 2009): Tc = 38 K at 150 GPa, 82 K at 300 GPa (Xie & Oganov, 2013).**
- **LiH_8: Tc = 31 K at 150 GPa.**
- **Tc = 81 K for SnH_8 at 220 GPa, 93 K for SnH_{12} at 250 GPa, 97 K for SnH_{14} at 300 GPa (Davari & Oganov, 2016).**

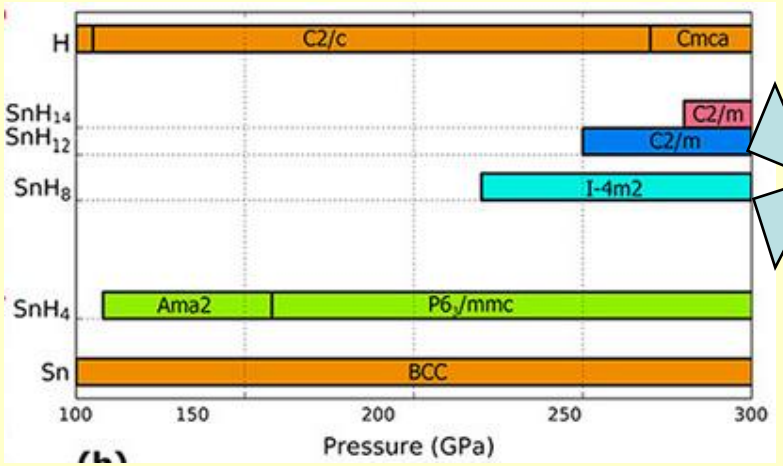

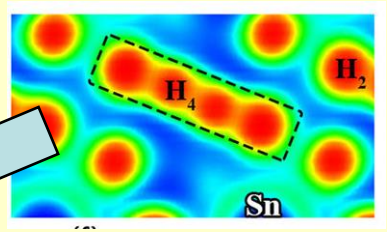

H_4-groups

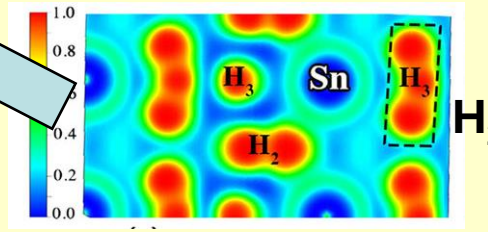

H_2, H_3-groups

New materials for fluorine storage

Cs-F

- CsF_2, CsF_3, CsF_5 are stable at 1 atm and can be used for storing and transporting fluorine.
- Decompose at 250-400 K.
- US patent.

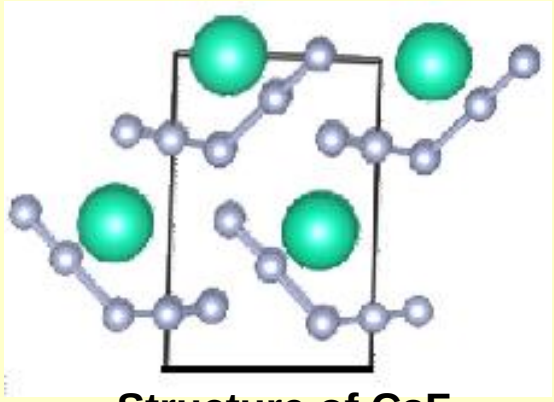

Structure of CsF_5 stable at 1 atm

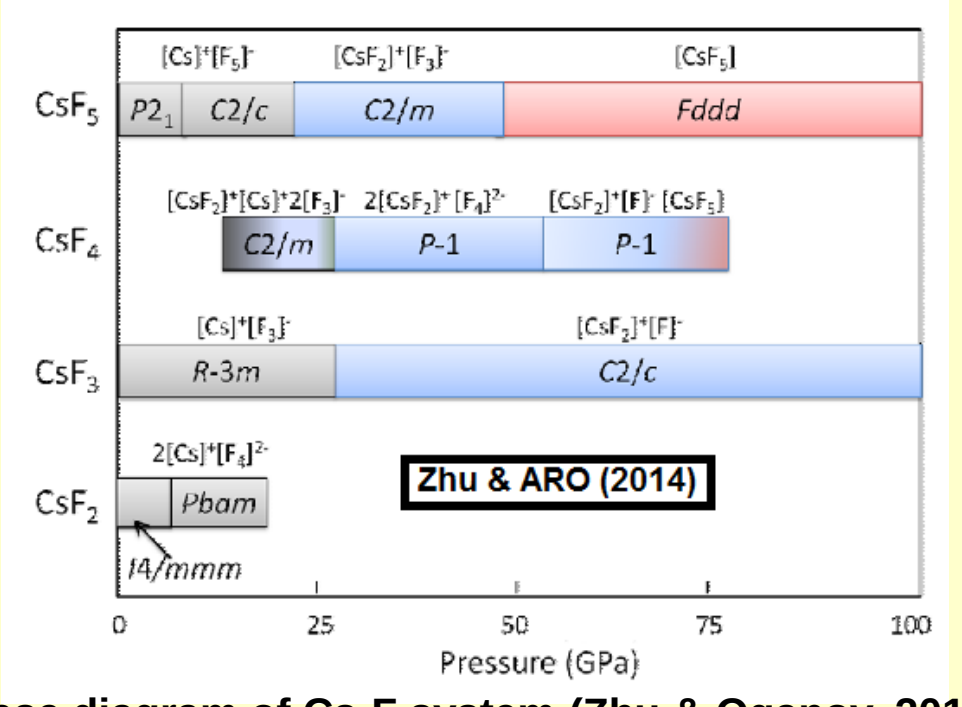

Phase diagram of Cs-F system (Zhu & Oganov, 2014)

[Zhu & Oganov, *Scientific Reports* (2015)]

B

2D-boron: prediction and synthesis

2013: prediction of buckled 2D-allotropes of boron with distorted Dirac cones (Zhou & Oganov, *Phys. Rev. Lett.* 2013).

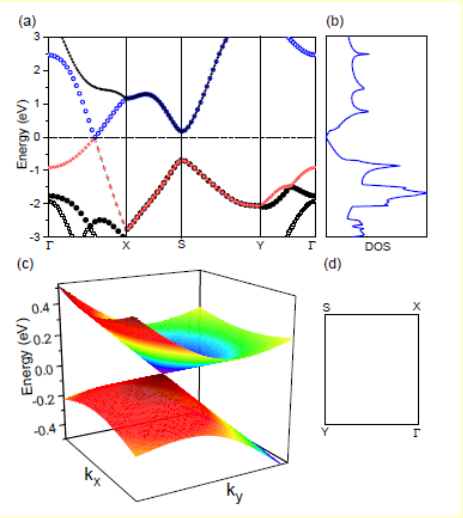

2015: synthesis of buckled B-monolayers on Ag-substrate (Mannix, Zhou, Oganov, *Science* 2015).

2D-boron – anisotropic metal with interesting properties:

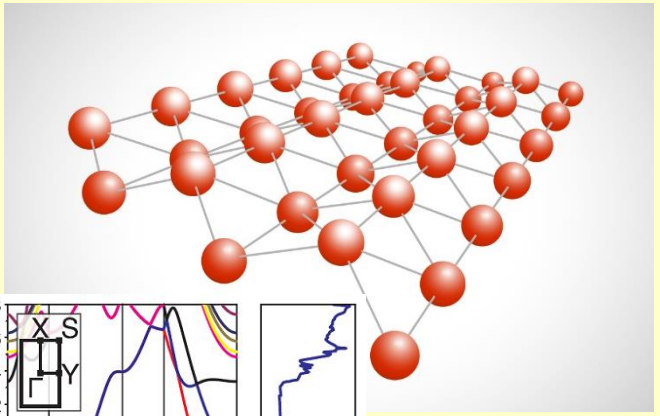

<u>Young's modulus</u> along *a* and *b*: 398 and 170 GPa*nm (graphene: 340 GPa*nm).
<u>Poisson ratio</u>: -0.04, -0.02.

<u>Superconductivity:</u> for 2D-borons predicted Tc up to 28 K (Zhao, *PRB* 2016).

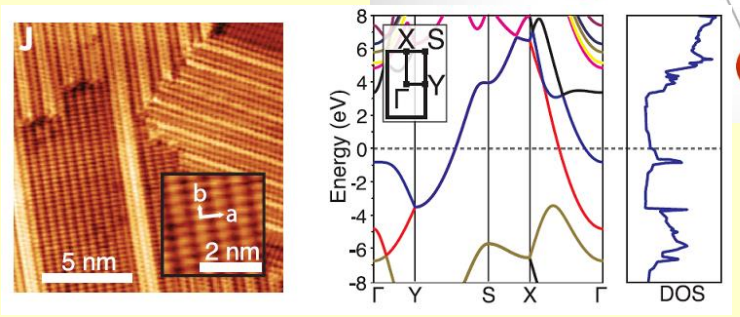

Surface stability depends on the chemical potential

$$E_{\text{formation}} = E_{\text{total}} - E_{\text{ref}} - \sum_i n_i \mu_i$$

$$E_{\text{formation}} = E_{\text{tot}} - E_{\text{ref}} - n_{\text{B}} E_{\text{AB}} - \mu_{\text{A}} (n_{\text{A}} - n_{\text{B}})$$

$$E_{\text{AB}} - E_{\text{B}} \leq \mu_{\text{A}} \leq E_{\text{A}}$$

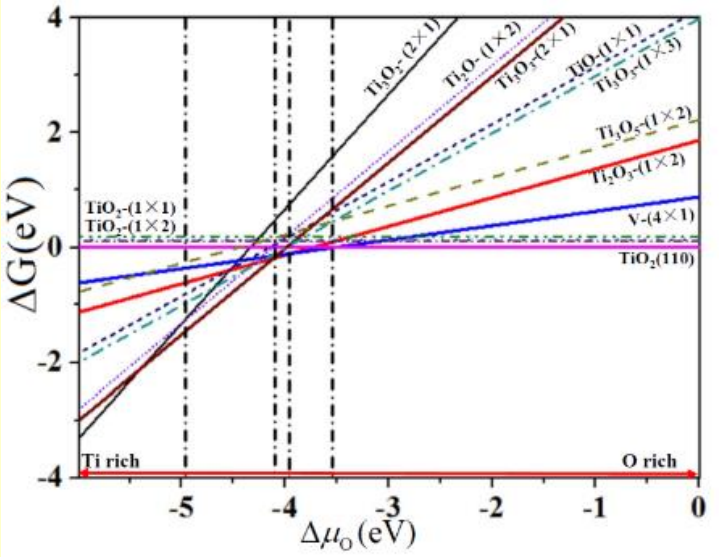

Energies of rutile (110) reconstructions as a function of chemical potential of oxygen (Wang, Oganov, Phys. Rev. Lett. 2014)

Surfaces of materials – new chemistry in 2D

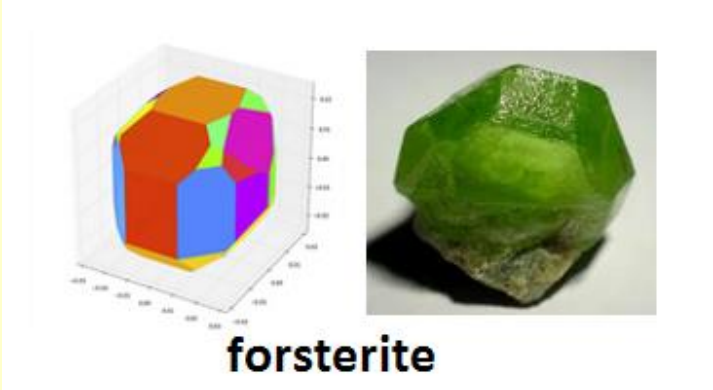

Surface energies and equilibrium crystal morphology – rapid prediction with quantitative periodic bond chain approach (Bushlanov & Oganov, in prep.)

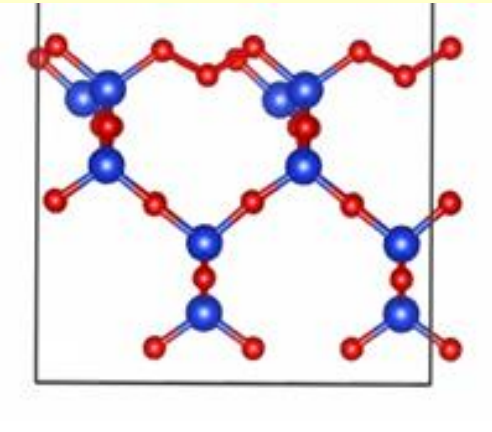

(001) surface structure of cristobalite SiO_2
(Feya & Oganov, in prep.)

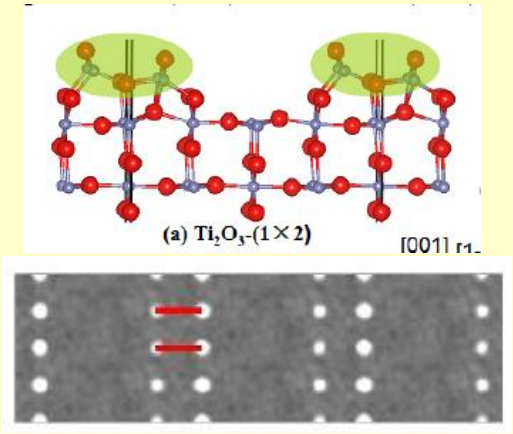

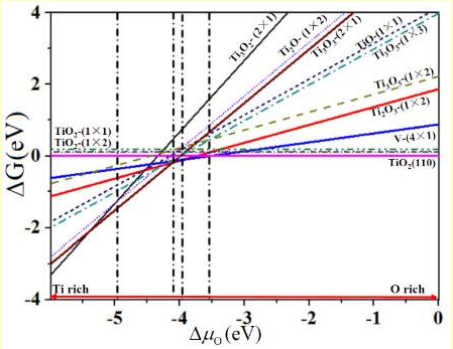

(110) surface structure of rutile (TiO_2)
(Wang & Oganov, *Phys. Rev. Lett.* 2014)

Prediction of new polymers with record-high dielectric constants

(Zhu, Sharma, Oganov: *J.Chem.Phys.* 2014, *Nature Commun.* 2014)

Nylon-6 test

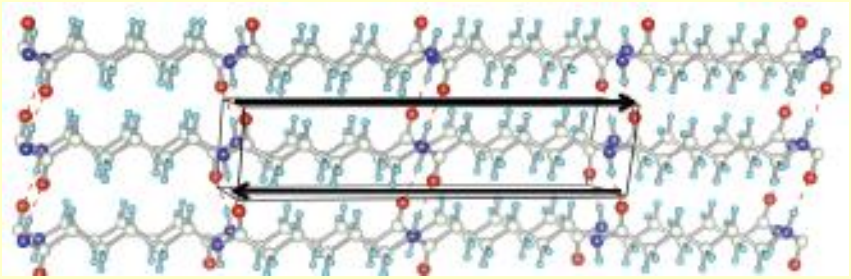

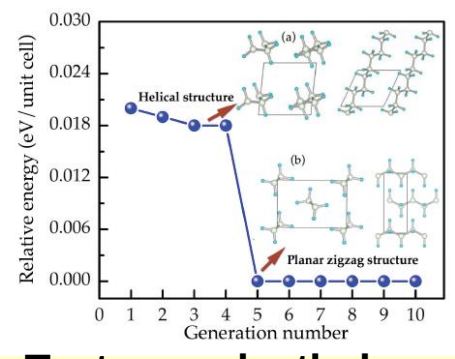

Test on polyethylene

Cellulose test

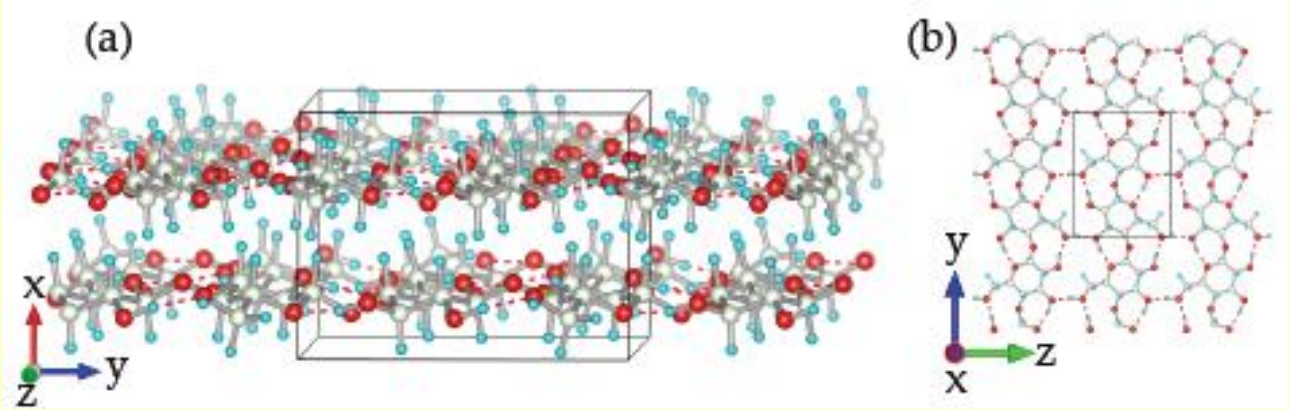

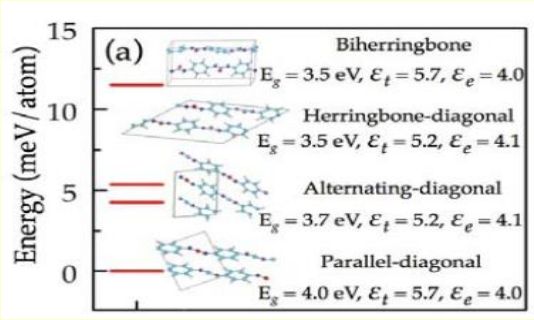

Prediction of 3 new high-k polymers

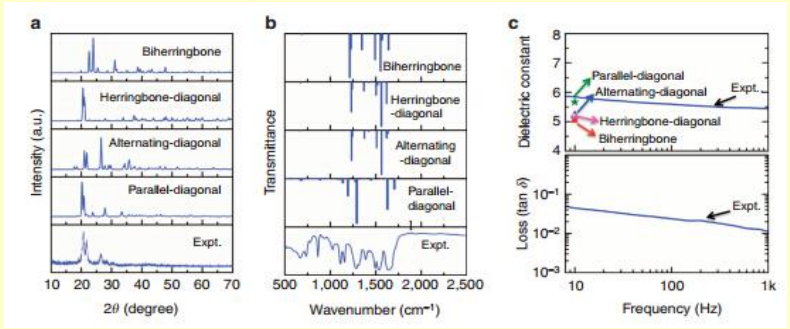

Experimental proof

0D-materials (nanoparticles) also display unexpected chemistry (Lepeshkin & Oganov, *Nanoscale* 2016)

Performance of USPEX and other methods for Lennard-Jones clusters (Lyakhov & Oganov, *Comp.Phys.Comm.* 2013)

Statistics for Lennard-Jones clusters with different algorithms. Best algorithms are highlighted in bold.

	Success rate (%)	Average number of structures until global minimum is found	Dispersion	Number of calculations
LJ_{38} (PSO [48])	100	605	N/a	100
LJ_{38}(USPEX)	**100**	**35**	**58**	**183**
LJ_{38} (EA [46])[b]	N/a	1265	N/a	100
LJ_{38} (MH [46])[b]	100	1190	N/a	100
LJ_{38} (EA [47])[b]	N/a	~2000[a]	N/a	N/a
LJ_{38} (PSO [48])	100	1649	N/a	20
LJ_{55} (PSO [48])	100	159	N/a	100
LJ_{55}(USPEX)	**100**	**11**	**30**	**60**
LJ_{55} (EA [46])[b]	100	100	N/a	100
LJ_{55} (MH [46])[b]	100	190	N/a	100
LJ_{75} (PSO [48])	98	2858	N/a	50
LJ_{75}(USPEX)	**100**	**2145**	**2024**	**53**

PSO = Particle Swarm Optimization
MH = Minima Hopping
EA = Evolutionary Algorithm

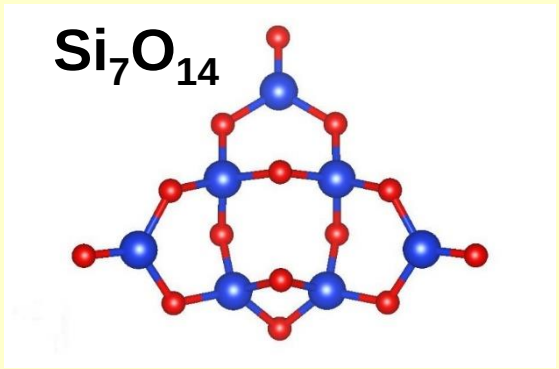

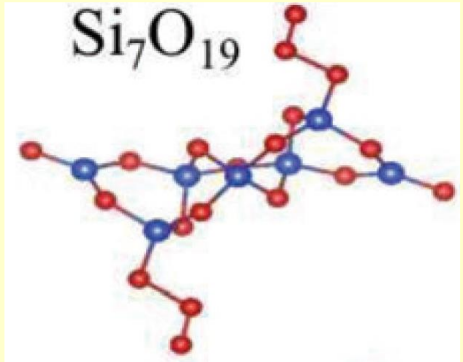

Ozonide-groups!
Dominant at T=300 K, $P(O_2)$=1 atm

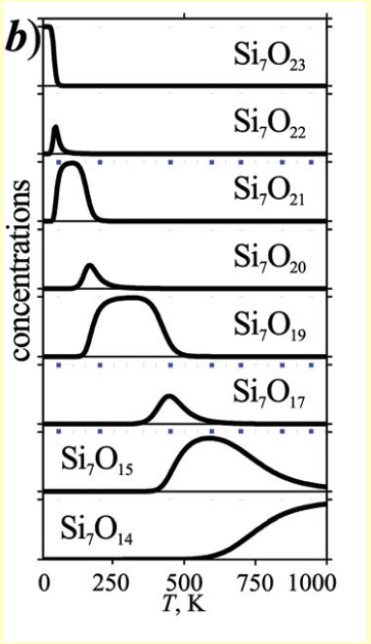

Predicted abundances of nanoparticles

Where are the limits?

-Maximum complexity of the system? ->About 100-150 atoms, periodic ordered structures

-Speed of *ab initio* calculations is prohibitive for large systems & finite-temperature predictions -> Machine learning!

-Prediction of synthesis? -> Sometimes

Generalized evolutionary metadynamics (GEM): solved structure of $Li_{15}Si_4$ with 152 atoms/cell

Li-Si

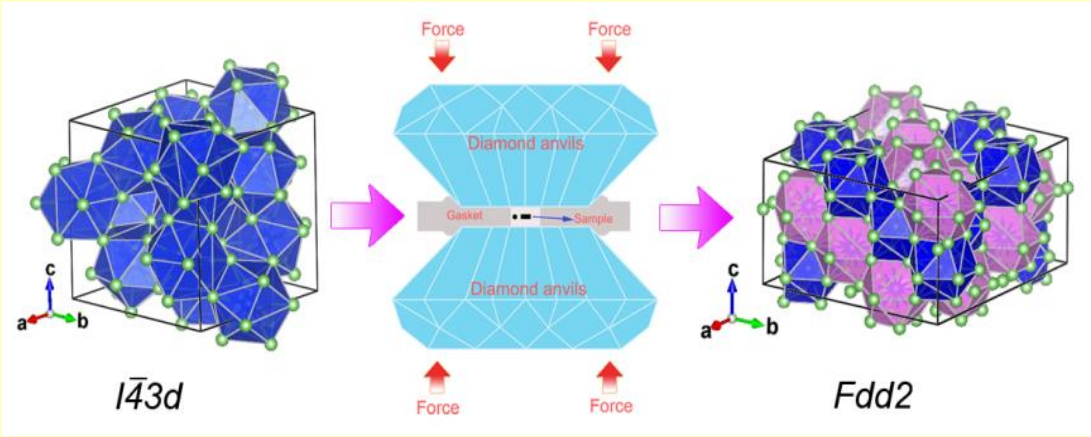

Structural transformation of $Li_{15}Si_4$ at 7 GPa. New phase has more attractive properties for use in Li-batteries.

Evolutionary metadynamics is a hybrid of:
-Metadynamics (Martonak, Laio, Parrinello, PRL 2003)
-Evolutionary algorithm USPEX (Oganov & Glass, JCP 2006)

It includes q-vectors and allows system size to change spontaneously

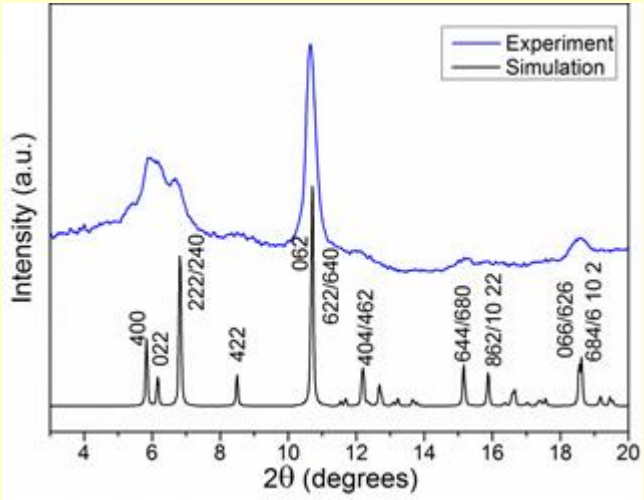

XRD of *Fdd*2-$Li_{15}Si_4$ at 18 GPa

[Zeng & Oganov, *Adv. Energy Mat.*, 2015]

GEM predicts new silicon allotrope with direct band gap of 1.28 eV, and possible path of its synthesis

(Zhu & Oganov, PRB 2015)

Si

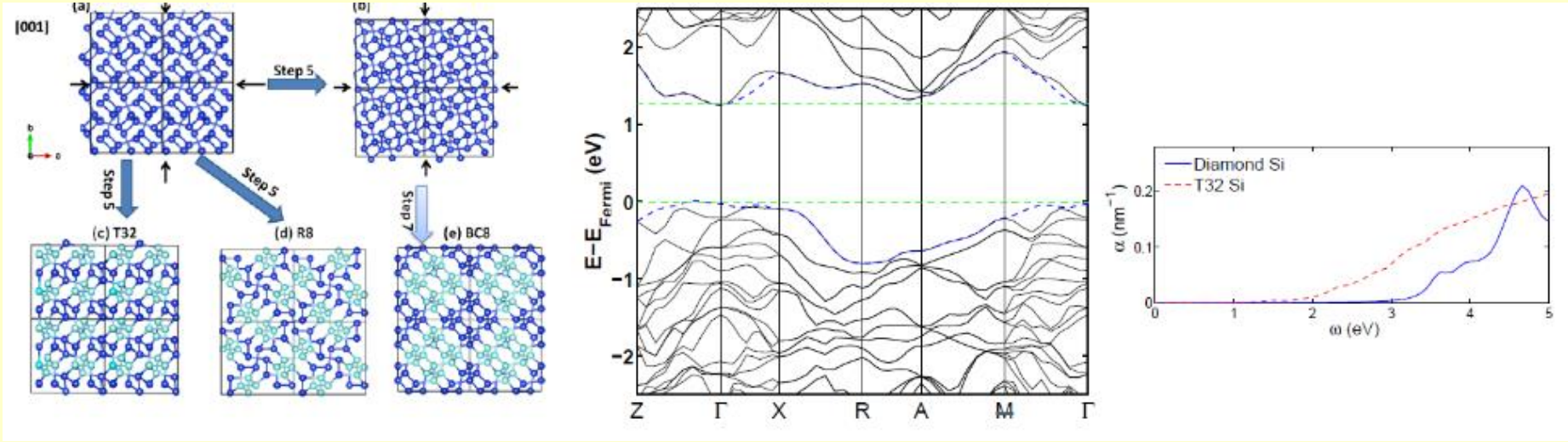

- **T32-Si was predicted by GEM calculations.**
- **Can be obtained by decompression of Si-II.**
- **Energy-degenerate with R8-Si.**
- **Absorbs solar spectrum much better than Si-I.**

- **Synthesized by A. Rode (*Nature Commun.*, 2015).**

Machine learning for accurate representation of high-dimensional potential energy surfaces

Dolgirev, Kruglov, Oganov (2016): combination of flexible pair potential and many-body potential described by a neural network.
Accuracy ~99.9%, speed ~100 times higher, compared to *ab initio* calculations.
Pair potential contains valuable chemical information.

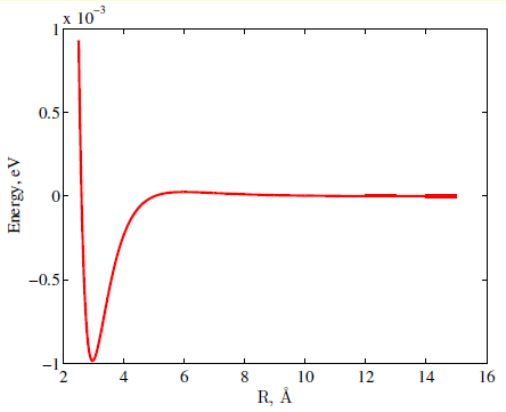

He-He potential
Σ(vdW radii)= 2.80 Å

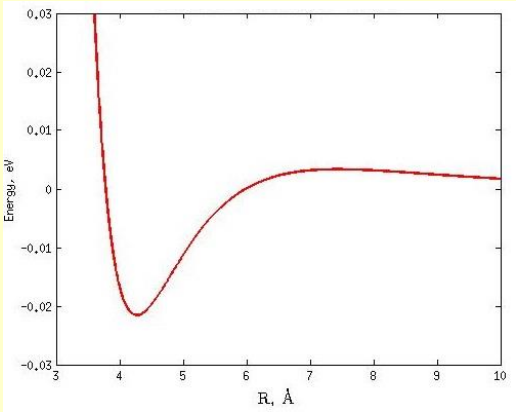

Xe-Xe potential
Σ(vdW radii)= 4.32 Å

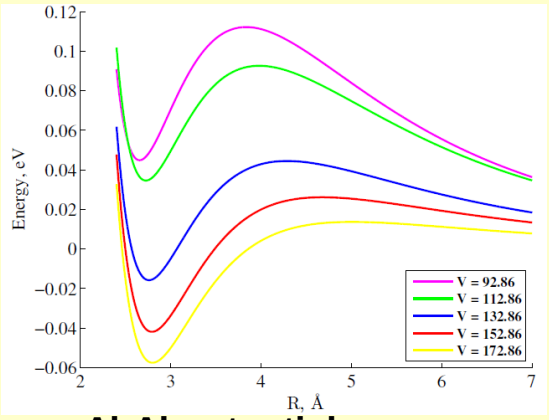

Al-Al potential
R(Al-Al) = 2.86 Å in crystal

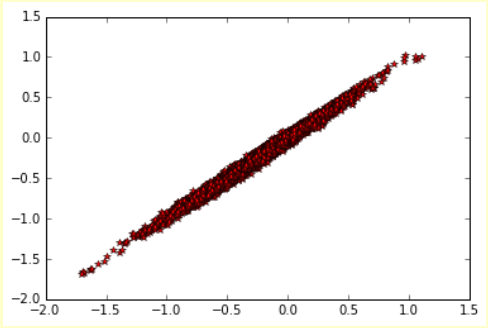

Comparison of forces from DFT and machine learning for Al, r>98%

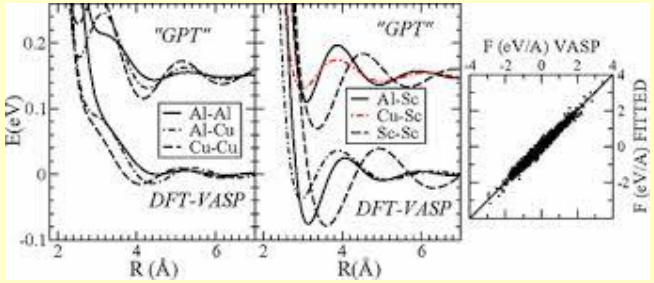

Typical Friedel oscillations in metals [Mihalkovic, *PRB* 2012]

Worst case for machine learning potentials is not too bad: carbon

Still, much better than reaxFF in the entire energy range:

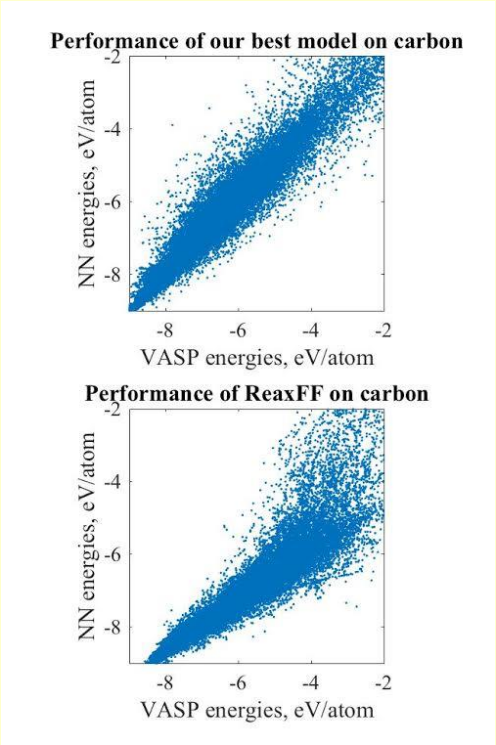

Test of NN and reaxFF accurary

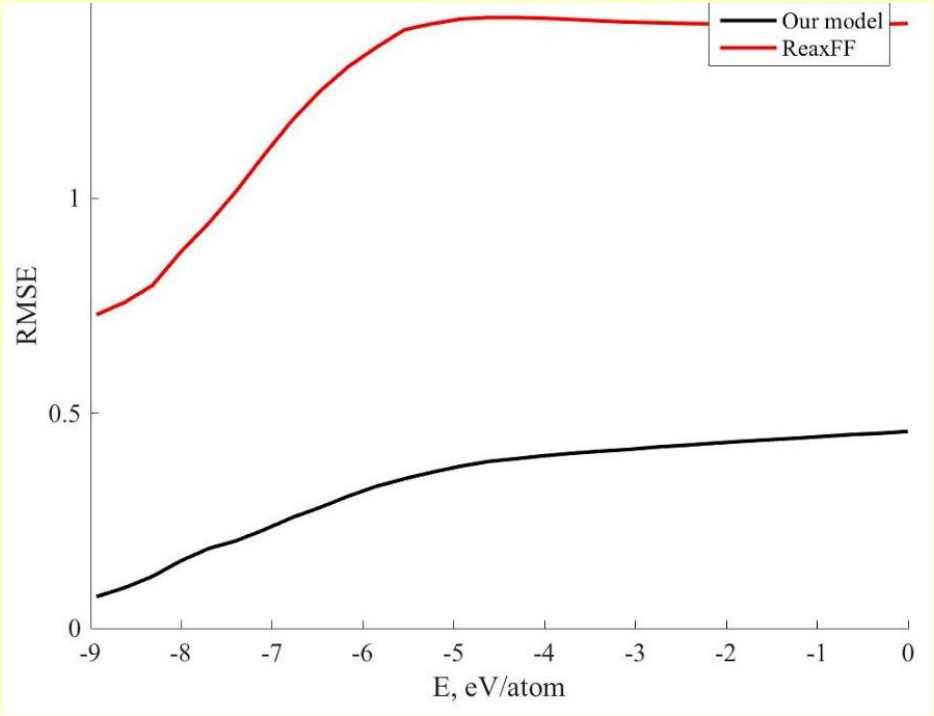

Comparison of RMSE across energy ranges

reaxFF potential:

A.C.T. van Duin, S. Dasgupta, F. Lorant and W.A. Goddard III, *J. Phys. Chem.* A, 105, 9396-9409 (2001)

Computer helps us to discover new science

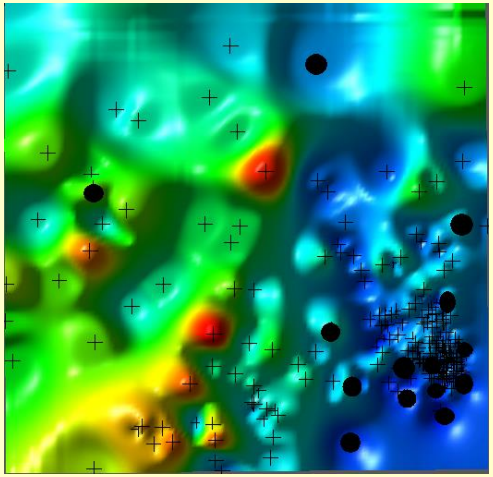

1. Predicting crystal structures by evolution

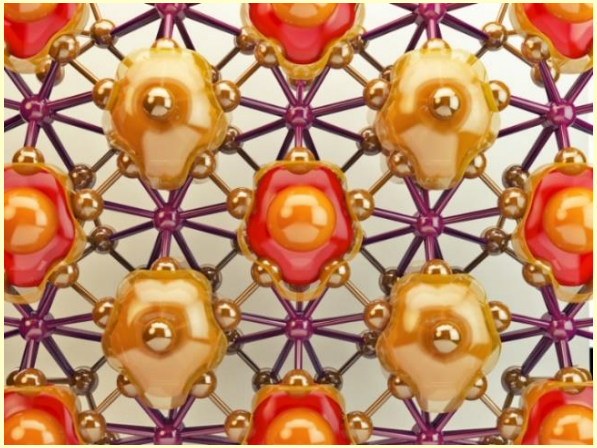

2. New materials and phenomena

Superhard materials
Superconductors
Li-battery materials
Photovoltaics
Magnets
Thermoelectrics

The team. Where great minds do NOT think alike

USPEX Computational Materials Discovery

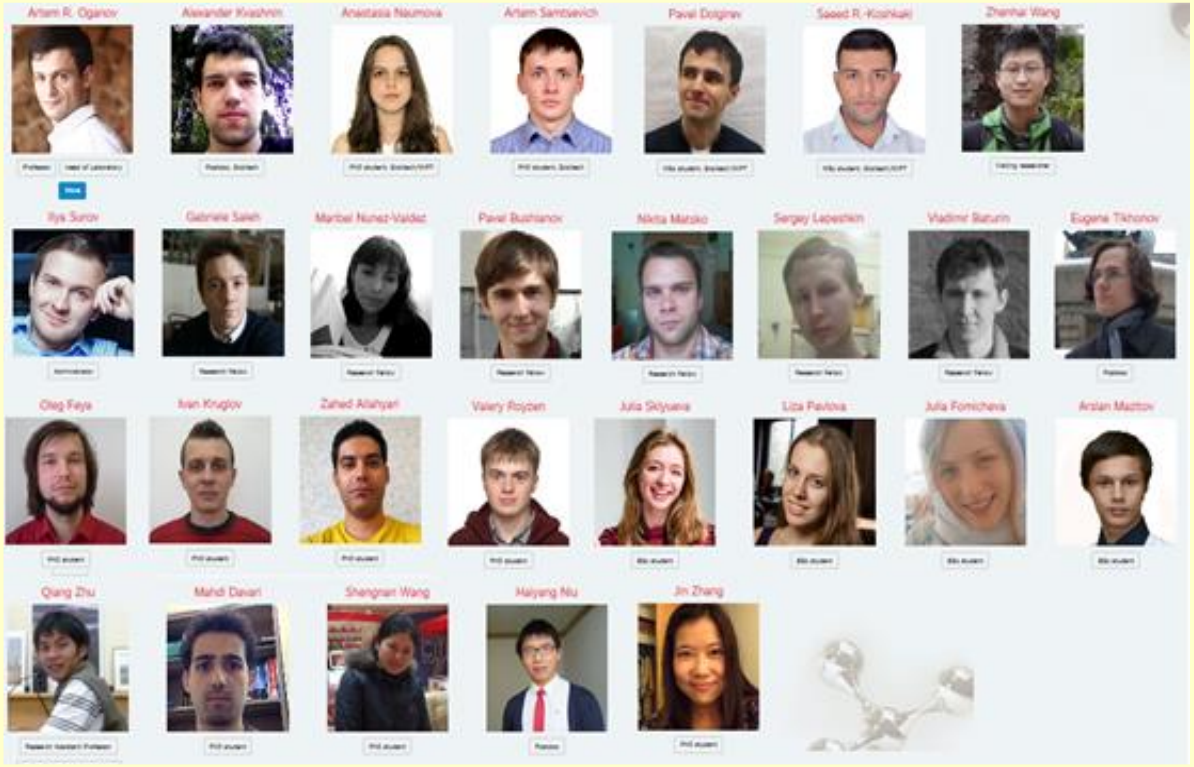

Experimental confirmation:

A. Goncharov

M. Eremets

USPEX can handle molecular crystals: New form of resorcinol

α

Space Group	P n a 2_1
Cell Lengths	**a** 10.4696(4) **b** 9.4062(3) **c** 5.6657(2)
Cell Angles	**α** 90 **β** 90 **γ** 90
Cell Volume	557.953
Z, Z'	**Z**: 4 **Z'**: 1

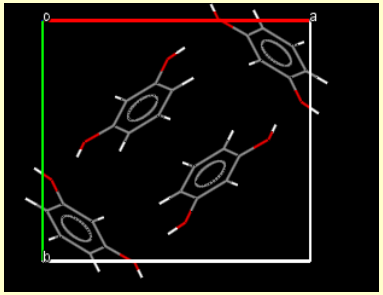

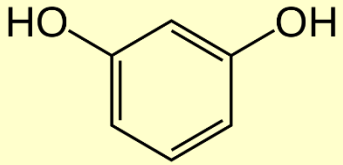

1934

2011

β

Space Group	P n a 2_1
Cell Lengths	**a** 7.934(2) **b** 12.606(2) **c** 5.511(1)
Cell Angles	**α** 90 **β** 90 **γ** 90
Cell Volume	551.188
Z, Z'	**Z**: 4 **Z'**: 1

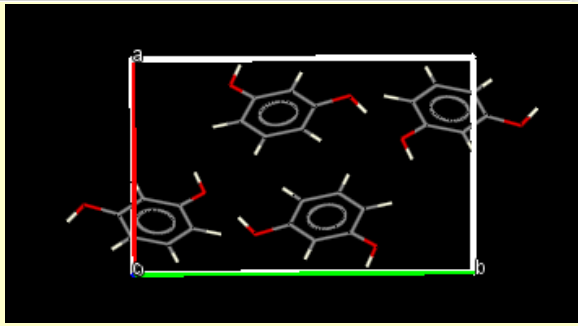

3rd phase of resorcinol from the melt with additives
Only PXRD is available, unable to solve

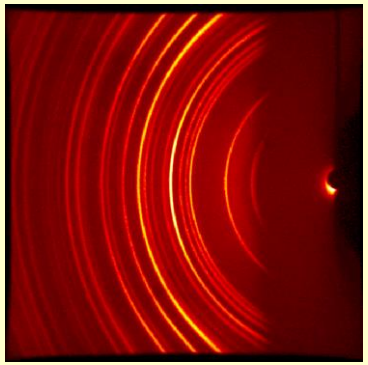

USPEX can handle molecular crystals: New form of resorcinol

Attempt #1: Z' = 1, found α and β,
no match to experiment

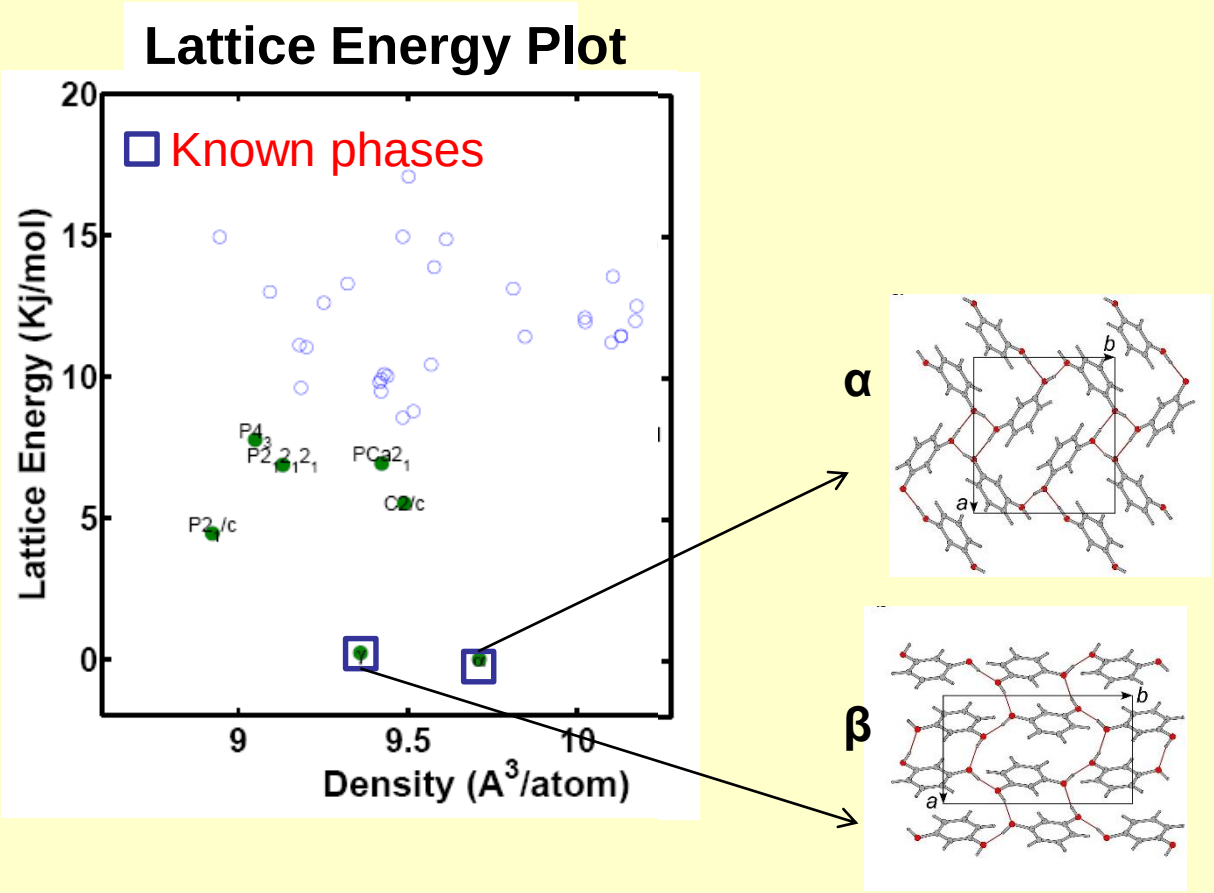

USPEX can handle molecular crystals: New form of resorcinol

Attempt #1: Z' = 1, found α and β

Attempt #2: Z' = 2, found γ !!!

Powder XRD comparison

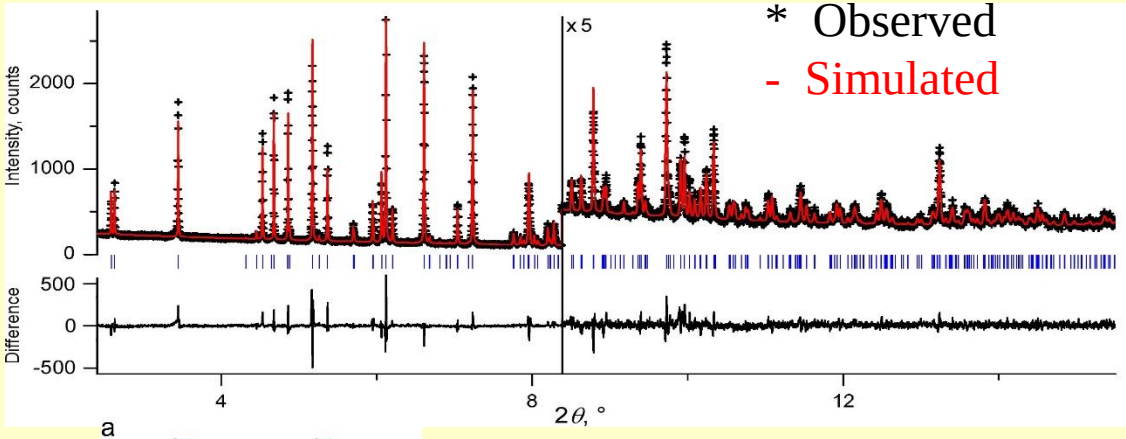

Lattice Energy Plot

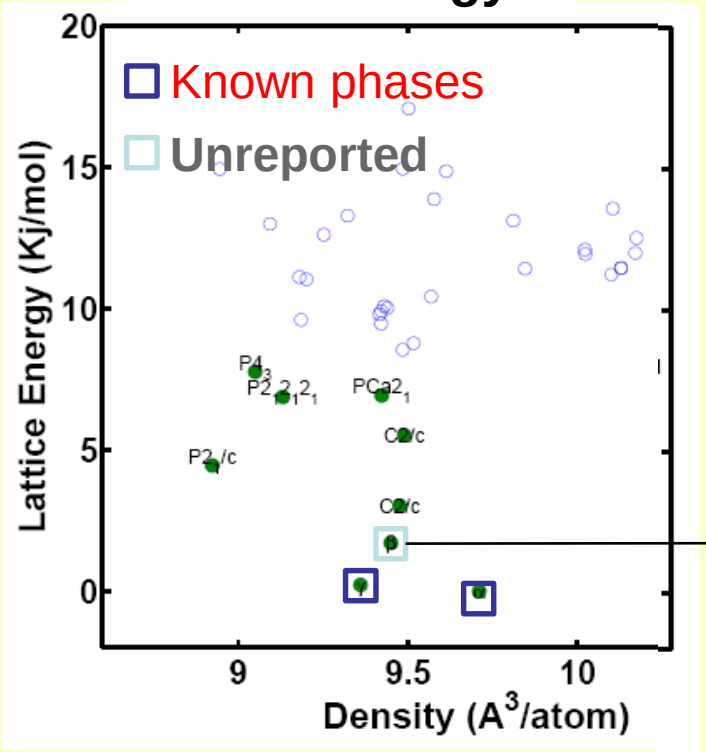

α

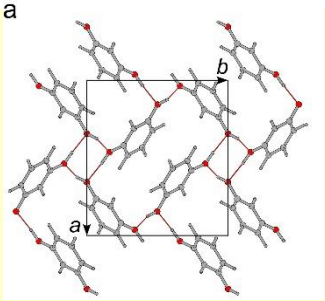

β

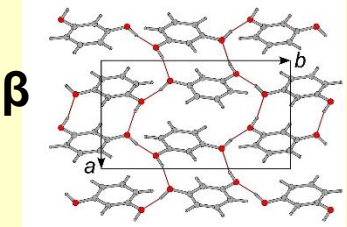

γ

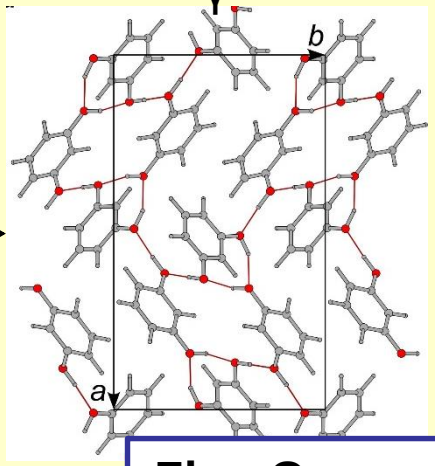

Zhu, Oganov, et al, JACS, 2016